

Chapter 7 Summary

This chapter describes vibration tests carried out using the test rig described in Chapter 3. The results are analysed and indicate a relationship between the peak angle of friction and rate of change of shear load/normal load ratio.

The measured angles of friction during sliding are lower than equivalent 'static' angles of sliding.

Chapter 7

Experiments using a vibrating test rig to measure the frictional resistance between rock surfaces.

7.1 Introduction

The vibrating test rig and associated analytical techniques described in chapter 3 and appendix 3 have been used to investigate friction between rock surfaces where the forces resulting in sliding are a combination of gravitational and inertial forces. The fundamental difference between these tests and those described in chapter 5 and 6 is the rate at which the applied forces are increased and decreased.

7.2 Purpose of the tests

Methods for designing slopes against vibrations have become more sophisticated in recent years since Newmark (1965) proposed the use of an analytical technique in which finite displacements are calculated for a given vibration record, (see chapter 3). Whatever design method is used, however, a representative value for the angle of friction (ϕ), must be obtained for the analysis. If friction varies with displacement then this too must be taken into account. For example Goodman and Seed (1966), showed, by laboratory experiments, that the displacements in a slope of cohesionless sand under vibration could be predicted when ϕ decreased with displacement in the same way as it did in direct shear tests. Further, that if initial peak values of ϕ had been used throughout the analysis the total slip would have been underestimated by 700%.

The experiments described here were designed to discover whether the frictional resistance developed by a rock discontinuity under a transient force is the same as that developed under a force which

changes more slowly (as in an inclined plane test or direct shear test).

7.3 Theory

The fundamental cause of friction between rock surfaces is still poorly understood except by analogy with metals, (see chapter 4). Adhesion at contact points is however, likely to be of importance along with resistance due to interlocking and ploughing of asperities. The relative importance of these two causes will depend upon the textures of the surfaces in contact.

Considering the results from inclined plane sliding for Darleydale Sandstone (chapter 5) where rock flour was removed between repeated runs, it was seen that the angle of sliding dropped from a peak of 32° to a residual of 12.5° . It has been proposed that this drop in frictional resistance be due to the removal and rounding of asperities, hence reducing the resistance due to interlocking and ploughing. The resistance caused by adhesion became relatively more important as the surfaces became more worn. In all inclined plane tests involving repeated runs it was shown that the residual angles of sliding were functions of the previous history of sliding of the surfaces, i.e. the 12.5° residual angle reached for Darleydale Sandstone in one test was the lowest angle that could be reached by the abrasion of the two surfaces. Consider the residual value to represent the condition when asperities have become so rounded that they can no longer cause further wear to other asperities. If this is the case, the residual angle of 12.5° for Darleydale Sandstone is a function of adhesive forces plus some component due to the interlocking of asperities that can no longer be modified to an extent that will effect the strength of the surfaces. If this is not the case the surfaces could suffer further

polishing and the angle of sliding might approach the low angles of friction reported for very smooth surfaces of the harder component minerals of the sandstone; e.g. quartz and feldspar $\phi = 6^\circ - 8^\circ$, Horn and Deere (1962). It seems reasonable to make the assumption therefore that the component of shear strength due to adhesion (S_a) for Darleydale Sandstone is $S_a \approx N \tan 7^\circ$

Now if it is further assumed that resistance due to adhesion is directly proportional to the applied normal load throughout the test i.e. not decreasing with displacement, then considering the initial strength of the fresh surfaces, we may write

$$\text{Shear strength (S)} = \begin{array}{c} \text{component due to } (S_a) \\ \text{adhesion} \end{array} + \begin{array}{c} \text{component due } (S_r) \\ \text{to roughness} \end{array}$$

$$\text{and } S = N \tan 32^\circ = N \tan 7^\circ + N \tan R^\circ$$

Calculation gives a peak value for R° of 27° .

At the residual angle of sliding, R° drops to 6° : i.e.

$$S = N \tan 12.5^\circ = N \tan 7^\circ + N \tan 6^\circ.$$

If shear strength can be considered in this way then it is possible to predict to some extent the frictional resistance that might be developed under transient loads.

Peak Values for the Initiation of Sliding

In the vibration tests described here, the block was raised slowly into position as in the inclined plane sliding tests described in chapter 5. It can be assumed therefore, that the available shear resistance before vibrational forces were applied was the same as in an inclined plane sliding test, e.g. for ground surfaces of Darleydale Sandstone the available shear resistance

$$S = N \tan 33^\circ.$$

Therefore for a slope angle of 20° , a block of Darleydale Sandstone may be expected to begin to move when the horizontal acceleration reaches

about 0.23g - (see chapter 3, figure 3.3). This is, however, assuming that the operative shear strength of Darleydale Sandstone is the same for a rapidly applied force as it is for a more slowly varying force. Such an assumption cannot be made. It has been shown for various materials (including Darleydale Sandstone) that when a force is applied suddenly there is a time lag between applied stress and strain, (see Robertson, 1963), figure 7.1.

Shear strength is a function of normal load which implies a physical change of the contact region with applied load. Hence where the applied forces are changed rapidly as in the case of vibration testing, the reaction of the surfaces to the changing loads may be out of phase with the applied loads and hence failure may occur at a later time (and at higher acceleration) than would be suggested by simply considering the case of a static load of similar magnitude. Such an effect was seen in this series of tests and is discussed later.

Frictional resistance whilst the block is sliding

A number of authors have shown that static friction is dependant upon the time that the surfaces are in contact before shearing. According to Bowden and Tabor (1946), Coulomb (1785) noted this effect for wooden surfaces in contact. Dokos (1946) has observed a similar time dependance for friction between metal surfaces that is particularly important for very short time intervals - less than 0.1 sec, Rabinowitz (1965).

Recent work by Dieterich (1972) and Scholz and Engelder (1976) has shown similar behaviour for rock surfaces. Scholz and Engelder were able to relate this time dependance to the change in real area of contact with time.

In the case of a sliding block the period of contact between any two points on the surfaces is only momentary; hence frictional resistance

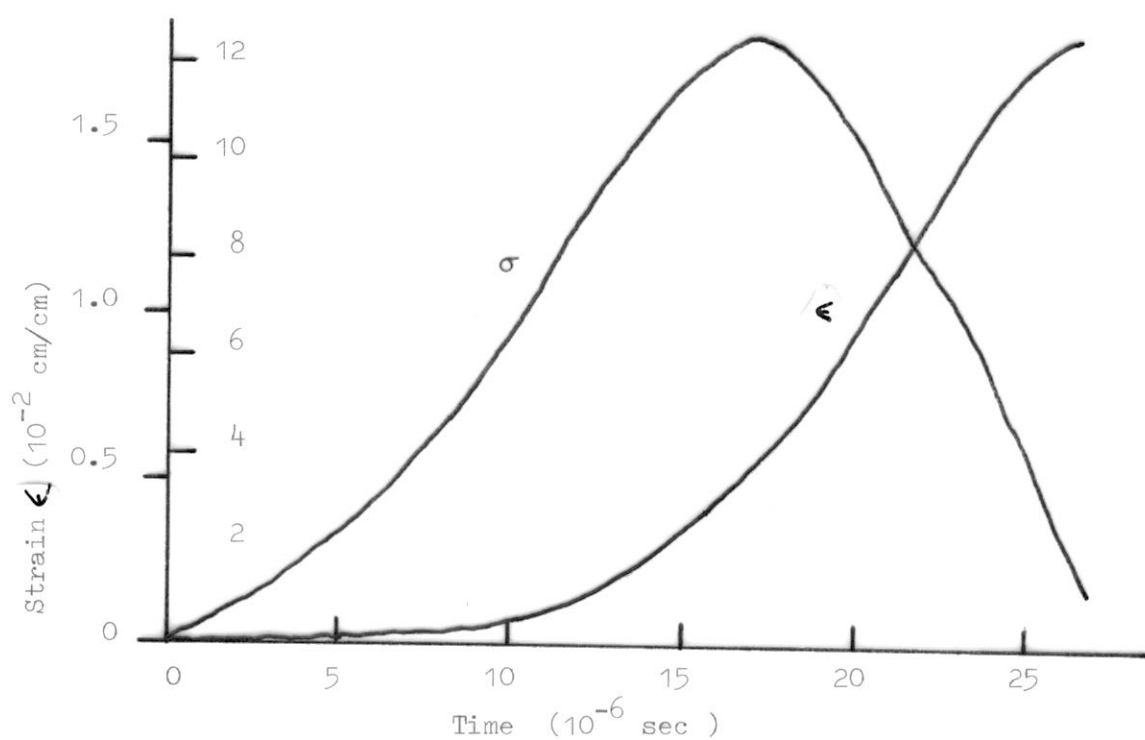


Figure 7.1 Time lag between applied stress and strain for an impact test on Darleydale Sandstone.

Redrawn from Robertson (1964), from original data of Attewell (1962)

will be lower than the resistance calculated using a 'static' friction value due to the relatively weak bonds that can be made whilst the block is moving. Lower values for 'sliding' friction were obtained from the experiments described here and are discussed later.

7.4 Description of tests

The following tests were carried out:

- 1) Tests using Portland Limestone sliders, (series B), in which runs were repeated on the same sliders either allowing rock flour to accumulate or removing flour between runs. These tests were designed to correlate with similar inclined plane tests described in chapter 5.
- 2) Tests (series C, D and E) were carried out using the other three rock types studied in previously reported sliding and direct shear tests (chapters 5 and 6). These tests consisted of two or three runs using the same slider and allowing rock flour to accumulate. Darleydale Sandstone was tested more fully than other rock types as the properties of this rock were better known from 'static' tests than those of others.

7.5 Procedure

The basal blocks and rock sliders were prepared in the same way as described in chapter 5. The top block chosen for these experiments was block no. M5, (see chapter 5, table 5.1). Inclined plane sliding tests had shown that less scatter in results occurred where heavier (metal) blocks were used. M5 was used rather than M4 because it was more squat and hence the vector sum of the gravitational and inertial forces was less likely to be directed outside the basal area of the block and therefore less likely to induce toppling (see section on

eccentricity, chapter 3).

For each test the required initial acceleration and frequency were determined and the necessary extension springs attached to the test rig, as explained in chapter 3. In most tests the initial acceleration used was approximately $0.4g$ with a frequency of about 3 Hz. These values for peak acceleration and frequency may represent ground vibrations from earthquakes of Richter magnitude 5.6 at 3 miles from the causative fault or Richter magnitude 7.6 at about 12 miles from the causative fault (see chapter 2, figures 2.10 and 2.8). Such a combination of high acceleration and low frequency are unlikely to occur due to standard production blasting.

The prepared top block was placed on the horizontal basal block on the edge closest to the camera, to avoid parallax effects, and the basal block then slowly raised to the angle of inclination required. Once the accelerometer had been calibrated with the chart recorder and film speed set at roughly 32f.p.s., (once at 64 f.p.s.), the chart recorder was started followed by the movie camera. The vibrating table was then released. When the block came to a halt or alternatively slid the complete length of the basal plane (16cm), the camera was stopped. The chart recorder was stopped after allowing the table to come almost to a halt so that a full vibration record was available for the accurate determination of the damping factor, k .

After each test the movie film was processed and each frame examined under a microscope to measure displacement values for both the block and table.

This data, along with data defining the acceleration record, was punched onto computer cards. The film data was matched in time with

the acceleration record, using the program TIMINGS (see chapter 3 and appendix 3) and analysed using the program EINSTEI. The program DISPLAC was then run for the same angle of slope and input vibration but for different values of ϕ across the range obtained from EINSTEI. The results from these two programs were then compared.

7.6 Results

Examples of typical results have been given in chapter 3 and others for run 2 of the same test are given here in figures 7.2, 7.3 and 7.4. These results are sufficient to illustrate the factors involved in the analysis of the tests but the results from all tests are available bound as an appendix to a companion volume of this thesis presented for the Diploma of Imperial College (D.I.C.) and held in the Watts Library, Department of Geology, Imperial College, London S.W.7. (Henchler, S.R. (1977) "The effect of vibration on the friction between planar rock surfaces", D.I.C. Thesis, (Imperial College) University of London.)

7.7 Discussion of results

The results from EINSTEI show considerable scatter, partly due to real variations in ϕ during sliding but mainly due to experimental reading errors. Even using the microscope reading errors were of the order of $\pm 0.1\text{mm}$. Additional errors, probably of the same order as reading errors, were introduced because of the finite exposure time of each film frame.

These errors are important for individual values for frictional coefficient but are less important when results are considered over all.

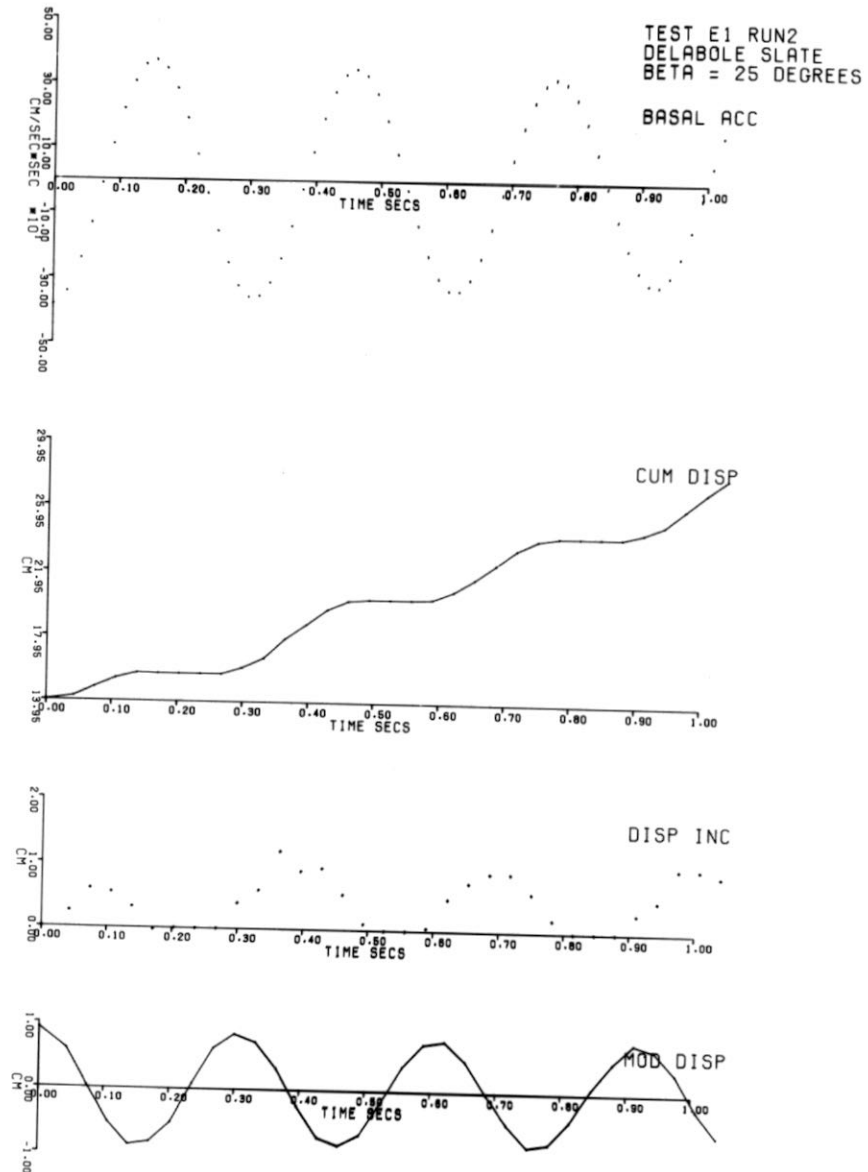


Figure 7.2

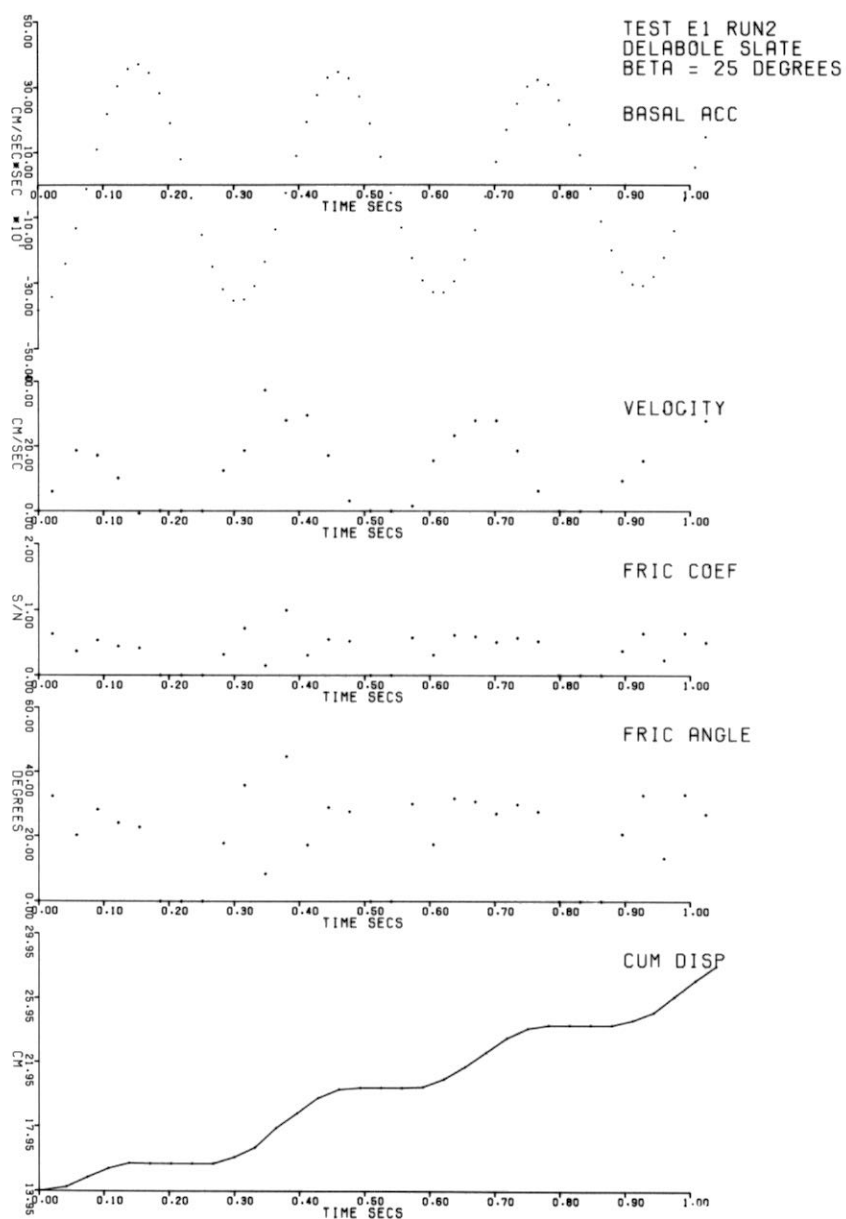


Figure 7.3

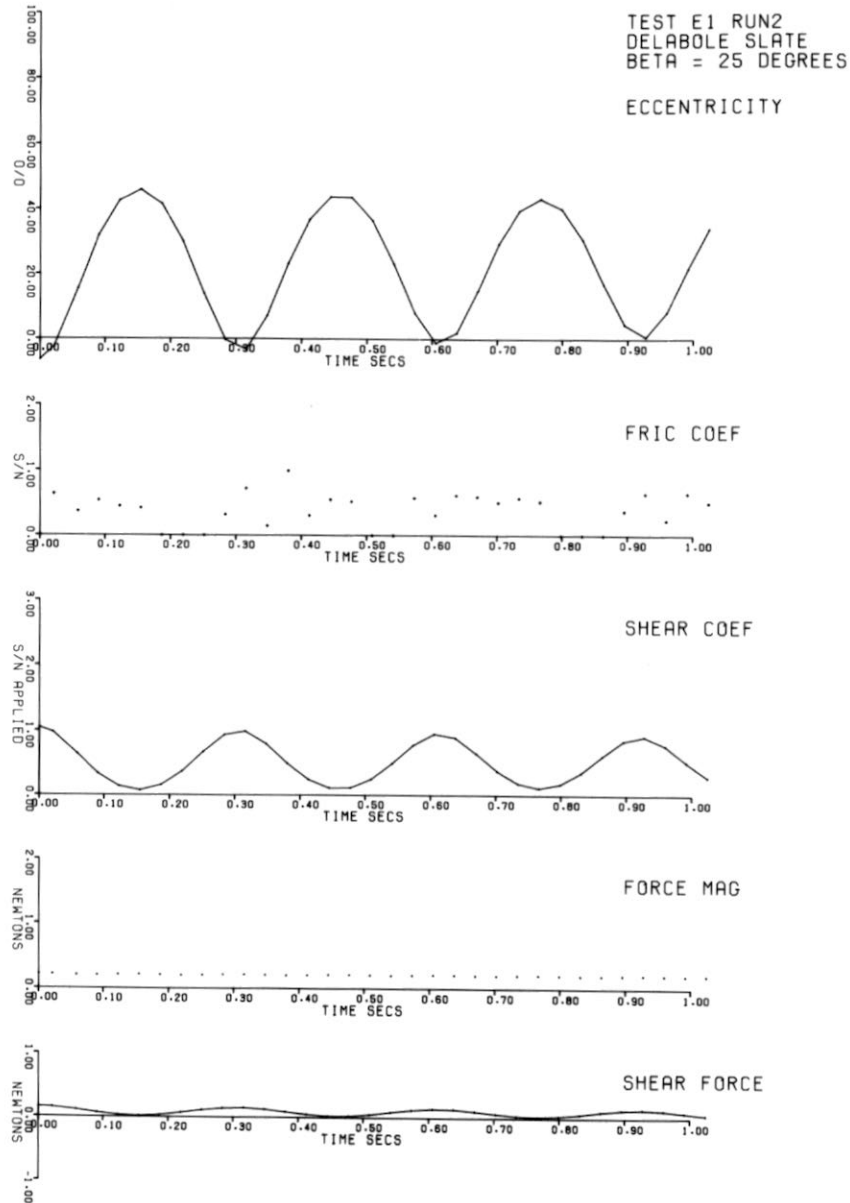


Figure 7.4

The problem is similar to that explained in chapter 3, concerning timing the experiment. For example, if between times t_1 and t_2 forces were acting that resulted in a real block displacement of 1.35mm, but this displacement was only measured as 1.2mm, then back calculation would produce a higher value for the frictional resistance than the correct one. If, in the next time interval the displacement was 1.0mm but was measured as 1.15mm (making up for the error in the previous measurement) then strength would be underestimated. The errors are not cumulative but tend to cancel out. A good example of this occurs in the results of test E1 Run 2 given in figures 7.2, 7.3, 7.4. In figure 7.2, in the graph of displacement increments (DISP INC) it is seen that at a time of about 0.37 secs, a large displacement increment of about 1.2cm was measured. Quite clearly this measured value is exceptional, within the pattern of this graph. The following value is small. A corresponding discrepancy can be seen in the velocity : time graph in figure 7.3.

The calculated value for friction coefficient (FRIC COEF) and friction angle (FRIC ANGLE) in the same figure reflect this anomolous result and show a very low value followed by a high value followed again by a low value.

The fact that an individual error can cause such a variation in calculated results for several time periods after the error occurred is due to the fact that each calculation of frictional coefficient relies upon the calculated velocity for the previous time increment.

The next cycle of displacement gave fairly constant friction values and in the last cycle there is again some variation due probably to reading errors.

By comparison the results given for test E1, Run 1 in chapter 3 give much more constant values for friction.

The fact that, where variation does occur, the errors tend to cancel one another out has led to the use of a statistical appraisal of the results. For example, the mean of the second group of friction angle values, (times 0.25 - 0.5 secs) from figure 7.3 is 25.82° ; the mean for the whole record is only slightly different, 26.24° , with a standard deviation of 7.98° .

The results for the whole of test E1 run 1 give a mean of 28.23° with standard deviation of only 3.9° . Partly on account of the scatter in results it is difficult to determine whether there is any relationship between friction and other parameters such as velocity of block.

In particular a relationship might have been expected between friction coefficient and eccentricity. However no such relationships are evident. A decrease in friction angle with displacement might be expected but the one or two degree variation over 16cm for surfaces with flour accumulating is too small to be separated from the scatter of data.

Results for tests are therefore analysed statistically, giving mean angles of friction and standard deviations. Results are plotted as histograms and cumulative frequency curves; these serve very well for comparing individual runs.

Tests investigating the reduction in friction with displacement.

Three tests were carried out using Portland Limestone sliders :

- i) TEST B1 consisted of two runs with an angle of inclination of 20° , allowing rock flour to accumulate.
- ii) TEST B2 consisted of 9 runs. The first 6 were carried out with an angle of inclination of 30° with rock flour accumulated between runs. Flour was removed before the seventh run and the

angle of inclination reduced to 25° . For 8 and 9 flour was again removed and the angle of inclination reduced to 20° .

iii) TEST B4, consisted of 17 runs, rock flour being accumulated over the first 14 runs, and removed for the last 3. The angle of inclination was decreased progressively throughout the test between runs, from 30° to 10° .

The results from test B1 are given in figure 7.5.

In figure 7.6 the results from the first six runs for test B2 in which flour was accumulated are presented separately from the last three runs in which flour was removed.

There is clearly a lowering of the mean angle of friction for the second of these two groups of results. In figure 7.7 histograms of the results from all runs in test B2 are presented separately.

Figures 7.8 and 7.9 are cumulative frequency and histogram plots of the results from test B4 in which rock flour was removed from the start of the test but accumulated for the last 3 runs. The cumulative frequency graph in particular is very revealing in showing the relatively high values of friction for the first run compared to later runs and in illustrating that the range of values for ϕ remains fairly constant regardless of absolute values.

Results in terms of mean angles of friction and standard deviation for tests B1, B2 and B4 are given in table 7.1. Also presented in this table are average values of ϕ for complete runs obtained from the program DISPLAC. The method used for obtaining these results has been given in chapter 3. It will be noted that in all cases with the single exception of test B2, run 9, the mean value of ϕ , (ϕ_m) is less than ϕ_{av} as calculated from DISPLAC. This result is significant and will be discussed in detail later.

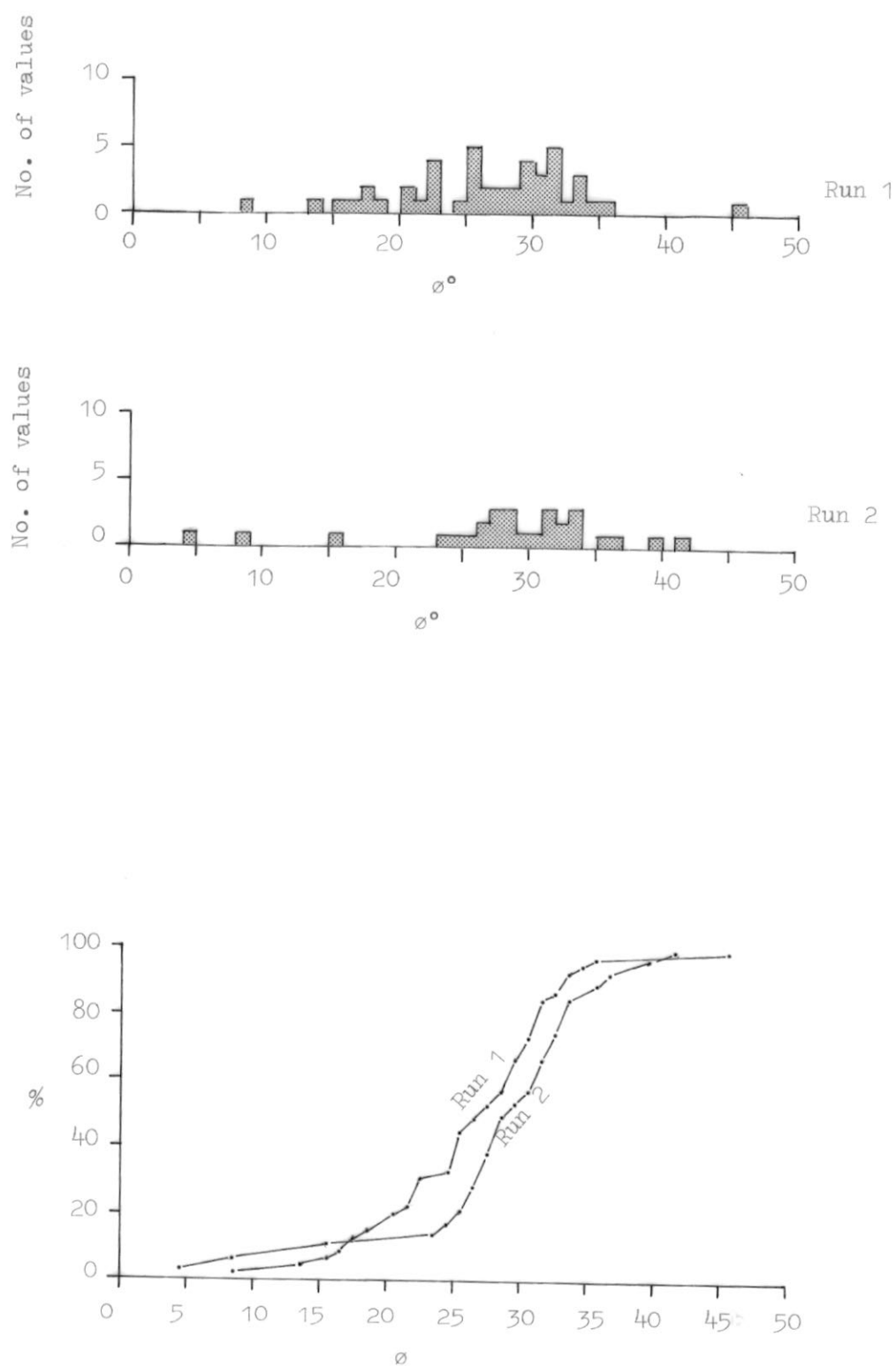


Figure 7.5 Test B1. Scatter histograms and cumulative frequency graphs for ϕ , runs 1 and 2.

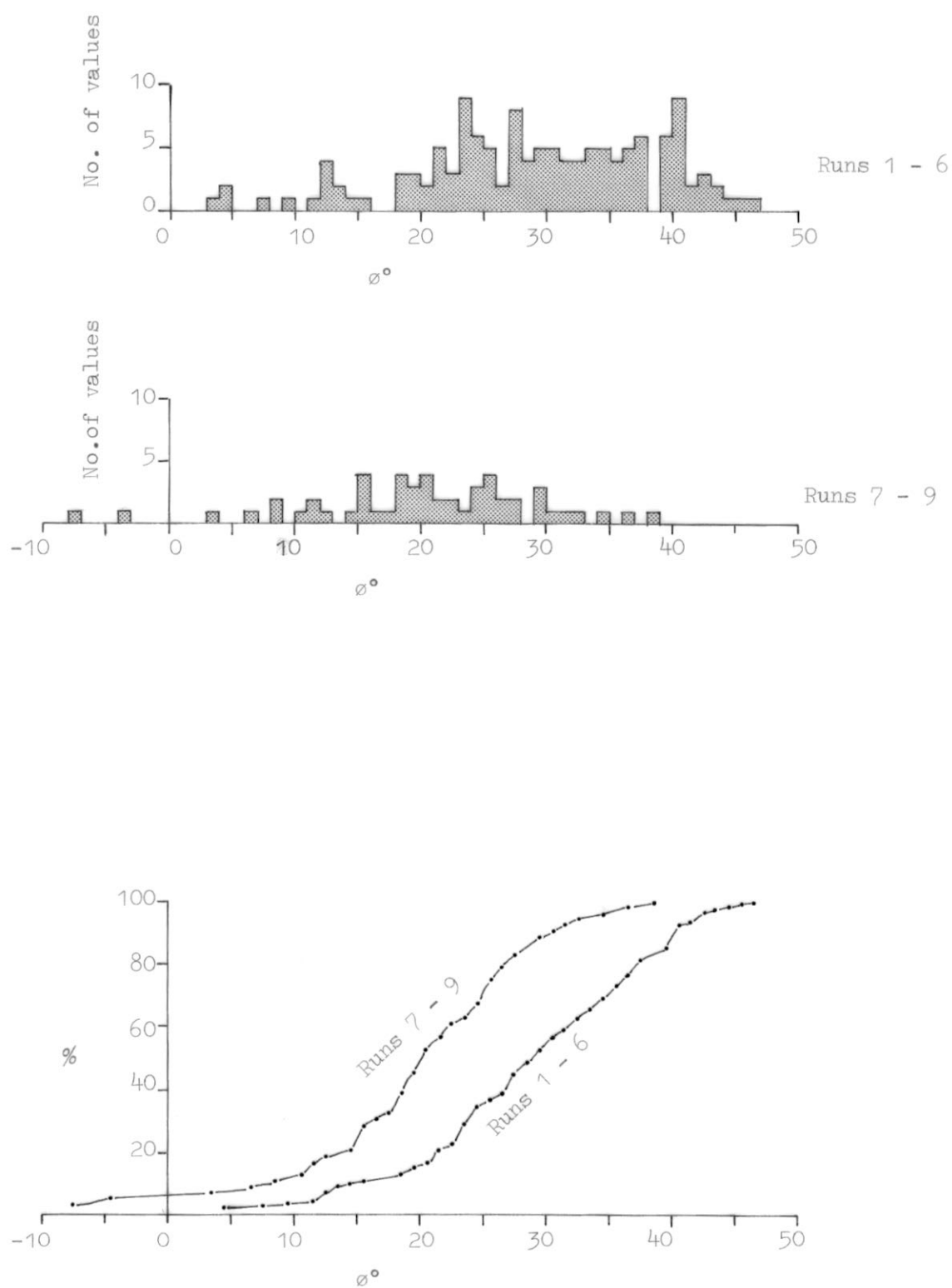


Figure 7.6 Test B2, Scatter histograms and cumulative frequency graphs for ϕ , runs 1 - 6 (flour accumulated), and runs 7 - 9 (flour removed).

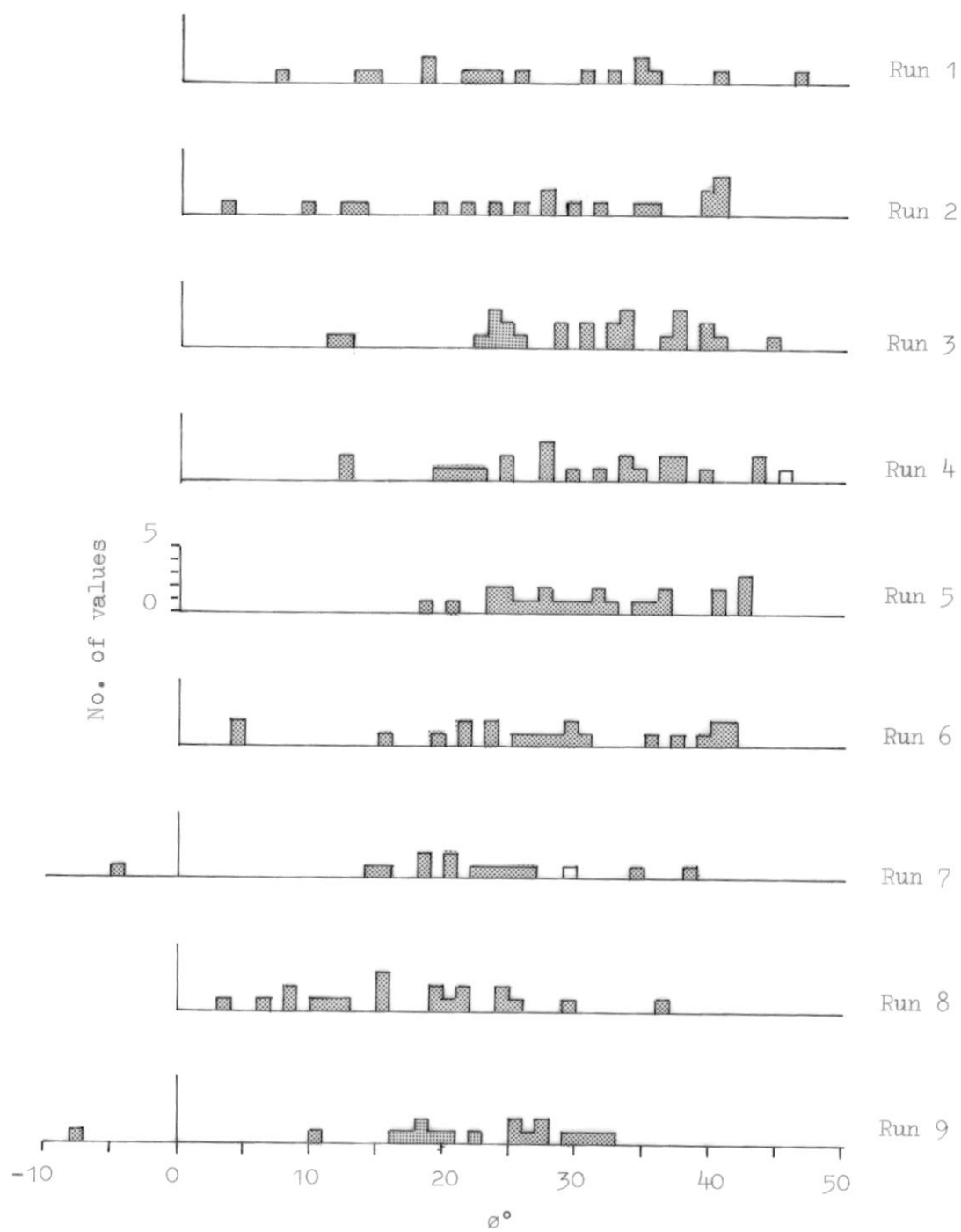


Figure 7.7 Test B2. Scatter histograms for \varnothing , individual runs.

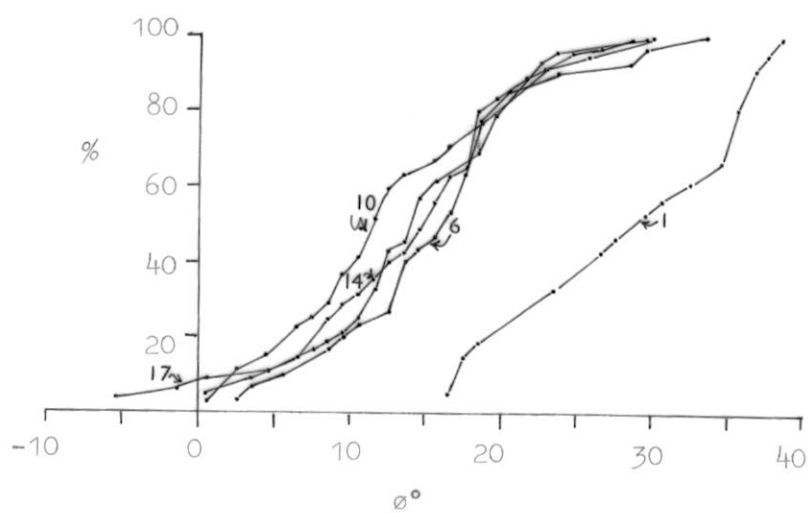


Figure 7.8 Test B4. Cumulative frequency graphs for runs 1, 6, 10, 14 and 17.

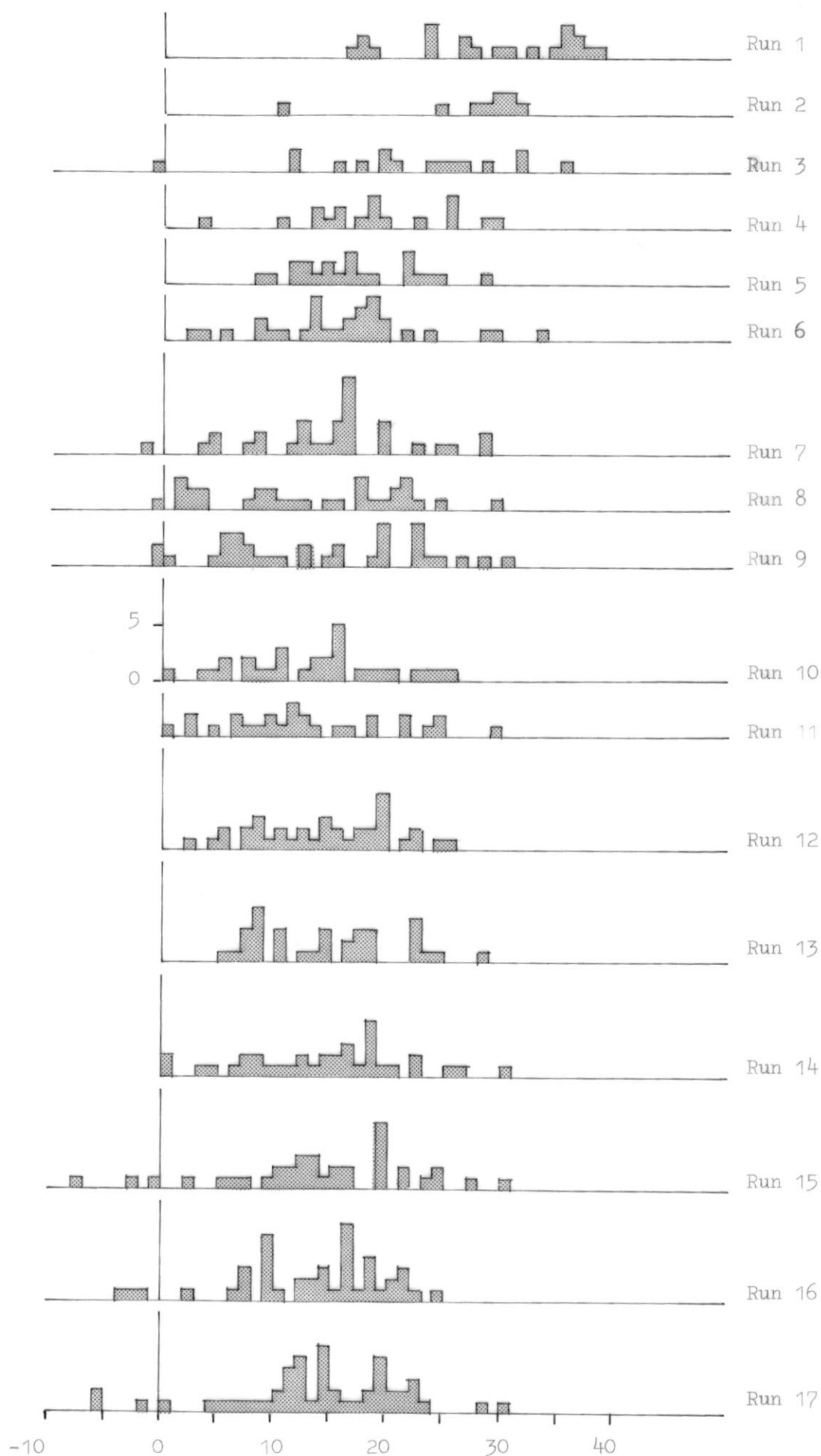
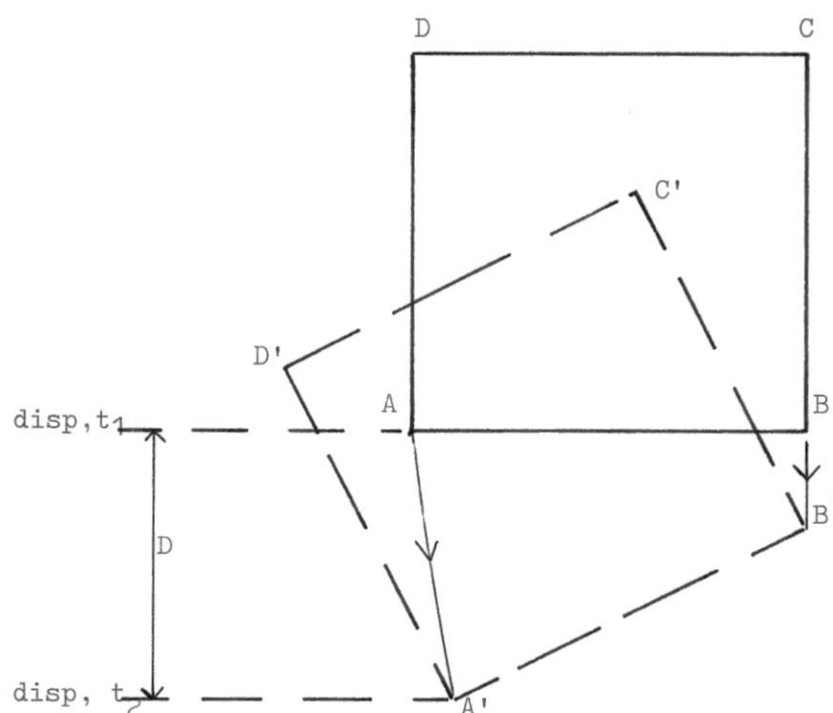


Figure 7.9 Test B4. Scatter histograms for ϕ , (individual runs)
Flour removed for first 14 runs.

Rotation

In many of these tests using Portland Limestone the block did not continue down slope in its original edge-forward position but rotated often by 45° to continue sliding corner forward, but occasionally by 90° so that a different edge faced down slope. The runs in which rotation occurred are indicated in Table 7.1. Clearly rotation of the block indicates a non uniform frictional resistance across the width of the block. If the frictional drag on one side is greater than on the other then one side will move at a slower velocity than the other and the block will swing around. The analysis of these rotationary movements in terms of the frictional resistance acting at different points of contact would be extremely difficult and would require a complete knowledge of the rotation history in plan. However it is important to consider the effect that these rotations may have on the calculated values for ϕ .



Consider the diagram on previous page. At time t_1 the block is in position ABCD and at time t_2 at A'B'C'D'.

The value of ϕ for this time interval as calculated using EINSTEI will depend on the measured value of displacement D (between the leading points of the block at times t_1 and t_2). Point A of the block moved a greater distance than D during this time, its displacement including a component of lateral movement. Hence the frictional resistance at that corner would be lower than that calculated using EINSTEI conversely the value at B will be higher than that calculated. Therefore, runs where rotation occurred are indicated and should be treated with some caution.

Rotation of blocks was an undesirable occurrence in these tests and it was necessary to consider why rotation occurred in some runs but not in others. Examination of table 7.1 and figures 7.10 and 7.11 reveal that rotation occurred under two conditions especially:

- i) in test B2 where flour was being accumulated;
- ii) in test B4 in the initial stages of sliding where the angle of friction was decreasing most rapidly.

It should also be noted that in four of the five cases where the block rotated in test B4, the calculated mean angle of friction was less than the angle of inclination, β , of the slope. This implies that the block would have slid even in the absence of vibration. Where the block is sliding so easily perhaps it is more prone to the effects of minor aberrations of the surface, causing spinning of the block.

These conclusions were not very useful in determining a way in which rotation might be avoided in later tests as these tests were to be similar in procedure to the first two or three runs of B2. One precaution taken was that the angle of slope β was kept at a lower angle than the probable value of ϕ_m . Rotation mainly occurred in tests using Portland Limestone.

Test No.	Run No.	Mean ϕ° ϕ_m	St. Deviation	ϕ average ^o from DISPLAC	β°	$\beta - \phi_m$	Rotation
B1	1	26.18	7.23	30	20	-6.18	R
B1	2	28.51	8.00	31	20	-8.51	R
B2	1	26.19	10.68	28	30	3.81	R
B2	2	27.10	11.43	29	30	2.91	R
B2	3	30.29	8.16	32	30	-0.29	R
B2	4	29.74	9.31	31.5	30	0.26	R
B2	5	31.12	7.12	32	30	-1.12	R
B2	6	27.71	10.68	32	30	2.29	R
B2	7	21.94	9.83	22	25	3.06	-
B2	8	17.52	8.36	19.5	20	2.18	R
B2	9	21.83	9.38	19	20	-1.83	-
B4	1	28.66	7.44	32	30	1.34	R
B4	2	26.99	6.44	27	30	3.11	R
B4	3	21.92	9.00	23	25	3.08	R
B4	4	18.77	6.93	19	20	1.23	R
B4	5	16.84	5.30	17	15	-1.84	R
B4	6	16.00	7.08	16.25	10	-6.0	-
B4	7	14.91	7.04	16.25	10	-4.91	-
B4	8	12.77	8.27	16.25	10	-2.77	-
B4	9	13.96	8.71	16.25	10	-3.96	-
B4	10	13.45	6.49	16.25	10	-3.45	-
B4	11	13.21	7.65	16.0	10	-3.21	-
B4	12	14.37	5.94	16.0	10	-4.37	-
B4	13	14.99	6.14	16.0	10	-4.99	-
B4	14	14.42	7.03	16.25	10	-4.42	-
B4	15	14.19	8.30	16.25	10	-4.19	-
B4	16	13.49	7.56	16.75	10	-3.49	-
B4	17	14.03	7.52	17.0	10	-4.03	-

Table 7.1 Tabulated results from tests B1, B2 and B3

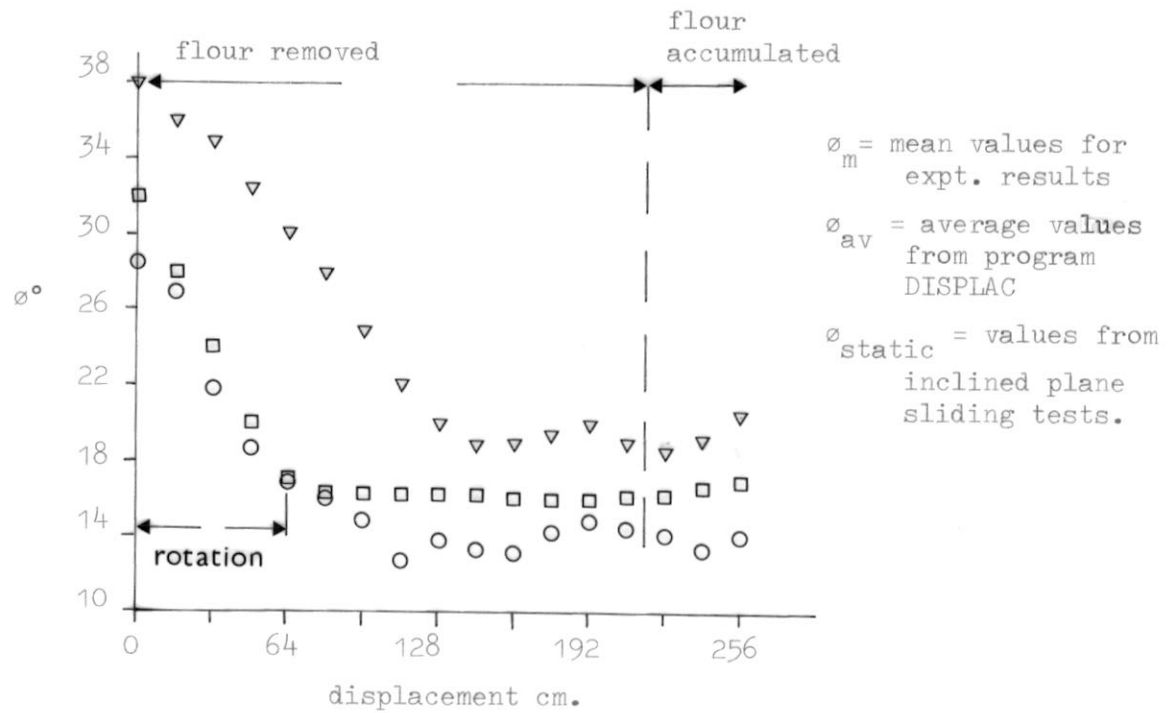


Figure 7.10 Comparison of vibration test (B4) results with inclined plane sliding results.

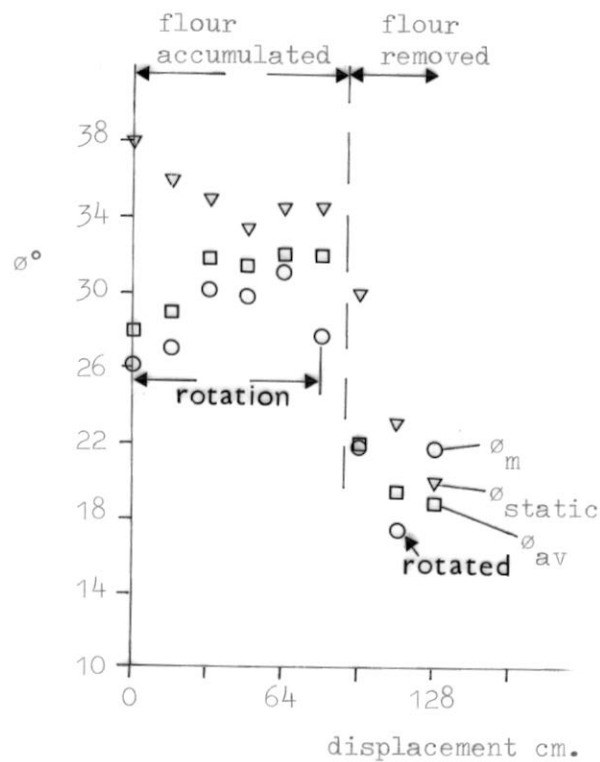


Figure 7.11 Comparison of vibration test (B2) results with inclined plane sliding results.

Comparison of values for ϕ_m , ϕ_{av} and ϕ_{static}

The results from tests B4 and B2 are presented graphically in figures 7.10 and 7.11. Figure 7.10 is a plot of the mean (ϕ_m) and average (ϕ_{av}) from DISPLAC) angles of friction versus displacement for test B4, in which flour was removed from the start. Also plotted in this graph are results from inclined plane sliding tests giving the peak angle of sliding (ϕ_{static}) versus displacement.

The last three points in each case are for runs in which rock flour was again accumulated. In the case of the inclined plane sliding test results (ϕ_{static}) flour was not, in fact, accumulated until after 288cm sliding (see figure 5.20).

Figure 7.11 gives the results of vibration test B2 compared to the corresponding tests using inclined plane sliding.

Two things are clear from these figures :

- i) ϕ_m and ϕ_{av} are much lower generally than ϕ_{static} ;
- ii) The shapes of the curves for vibration test results and inclined plane sliding results are similar.

The results for these and other rock types will be discussed in more detail later in this chapter.

Tests measuring values of friction for the first metre or so of displacement

Tests using Darleydale Sandstone, Permian Sandstone and Delabole Slate were carried out in the same way as for Portland Limestone. The number of runs in each test was restricted to either two or three. These tests are tabulated in table 7.2.

Five tests were conducted using Darleydale Sandstone sliders. Tests C1 and C2 both consisted of two runs with a slope inclination of 25°. The first run of test C1 was not filmed successfully. Tests

Test No.	Run No.	Mean ϕ° ϕ_m	St. deviation	β°	$\beta - \phi_m$	Rotation
C1	1	Film record lost				
C1	2	24.66	7.72	25	0.34	-
C2	1	27.92	7.76	25	-2.92	-
C2	2	25.94	7.43	25	-0.94	slight
C3	1	26.70	5.98	20	-6.70	slight
C3	2	27.67	4.51	20	-7.67	-
C3	3	27.60	5.46	20	-7.60	-
C4	1	27.97	6.46	20	-7.97	-
C4	2	28.08	5.36	20	-8.08	-
C4	3	27.62	5.00	20	-7.62	-
C5	1	25.01	17.39	22.5	-2.51	slight
C5	2	24.32	16.6	22.5	-1.82	slight
D1	1	23.88	7.95	25	1.12	slight
D1	2	24.07	6.53	25	0.93	slight
D2	1	24.55	5.46	20	-4.55	slight
D2	2	22.52	6.31	20	-2.52	slight
E1	1	28.23	3.90	25	-3.23	-
E1	2	26.25	7.98	25	-1.25	-
E2	1	27.39	5.62	20	-7.39	-
E2	2	27.07	5.60	20	-7.07	-

N.B. Average values for ϕ°_{av} from DISPLAC are given in table 7.3

Table 7.2 Data from vibration tests using Darleydale Sandstone, Permian Sandstone and Delabole Slate.

C = Darleydale Sandstone

D = Permian Sandstone

E = Delabole Slate

C3 and C4 consisted of three runs each with an angle of inclination of 20° . Test C5 consisted of two runs with an angle of inclination of 22.5° . This test was filmed using the camera's maximum frame speed (about 70 frames per second). The results of tests C1 to C4 are presented as histograms and cumulative frequency graphs in figures 7.12 to 7.14. Mean values for ϕ_m are given in table 7.2. The results from test C5 show a great deal of scatter due to the fast filming speed (see table 7.2), and hence histograms and cumulative frequency graphs are not given for this test as they are not meaningful. The camera was run at this fast speed in an attempt to improve film clarity. However, reading errors became proportionally greater for the smaller measured displacements.

This scatter, as in other tests, is self cancelling and the mean values of ϕ° obtained in this test do not differ greatly from those from other tests. In table 7.3 the average values for ϕ° obtained from DISPLAC are given. In these and subsequent tests values were obtained for intermediate times in the runs as well as the average value overall. For example, if in a test for a given table acceleration : time record, the block moved 4_{mm} in the first 0.5 sec, a value for ϕ_{av} is obtained which would give the same displacement in that time. From these results it is seen that ϕ_{av} varied only slightly during individual runs. Comparison of tables 7.2 and 7.3 shows that as with the results from tests using Portland Limestone ϕ_m was generally less than ϕ_{av} by one or two degrees.

Tests using Permian Sandstone (D1 and D2) and Delabole Slate (E1 and E2) were also carried out using inclined plans set at 25° and 20° . The results are given in figures 7.15 to 7.18 and in tables 7.2 and 7.3.

Test No.	Run No.	0.5 sec.	0.75 sec.	15 sec.	2 sec.	3 sec.	4 sec.
C1	2	26.5	26.25	26.0			
C2	1	29.5	29.25	29.0			
C2	2	27.0	27.25				
C3	1	29.0	29.0	29.0	29.25	29.5	29.5
C3	2	27.5	27.5	27.75	28.0	28.0	
C3	3	28.0	27.75	27.8	27.85	27.75	
C4	1	30.0	30.0	30.0	30.0		
C4	2	29.25	29.0	29.0	28.75	28.75	
C4	3	28.75	28.25	28.0	28.0	28.0	
C5	1	30.0	29.5	29.0	28.75		
C5	2	28.0	27.0	27.0	27.5		
D1	1	27.0	27.0	27.0			
D1	2	26.0	26.0	26.5			
D2	1	29.0	27.75	27.0	26.75		
D2	2	27.0	27.0	26.0	25.5		
E1	1	29.5	29.25	29.25			
E1	2	27.5	27.5				
E2	1	29.25	29.5	29.25	29.5	29	
E2	2	29.5	28.5	28.25	28.5	28.5	

Table 7.3 Average values of ϕ from DISPLAC for different times during each run.

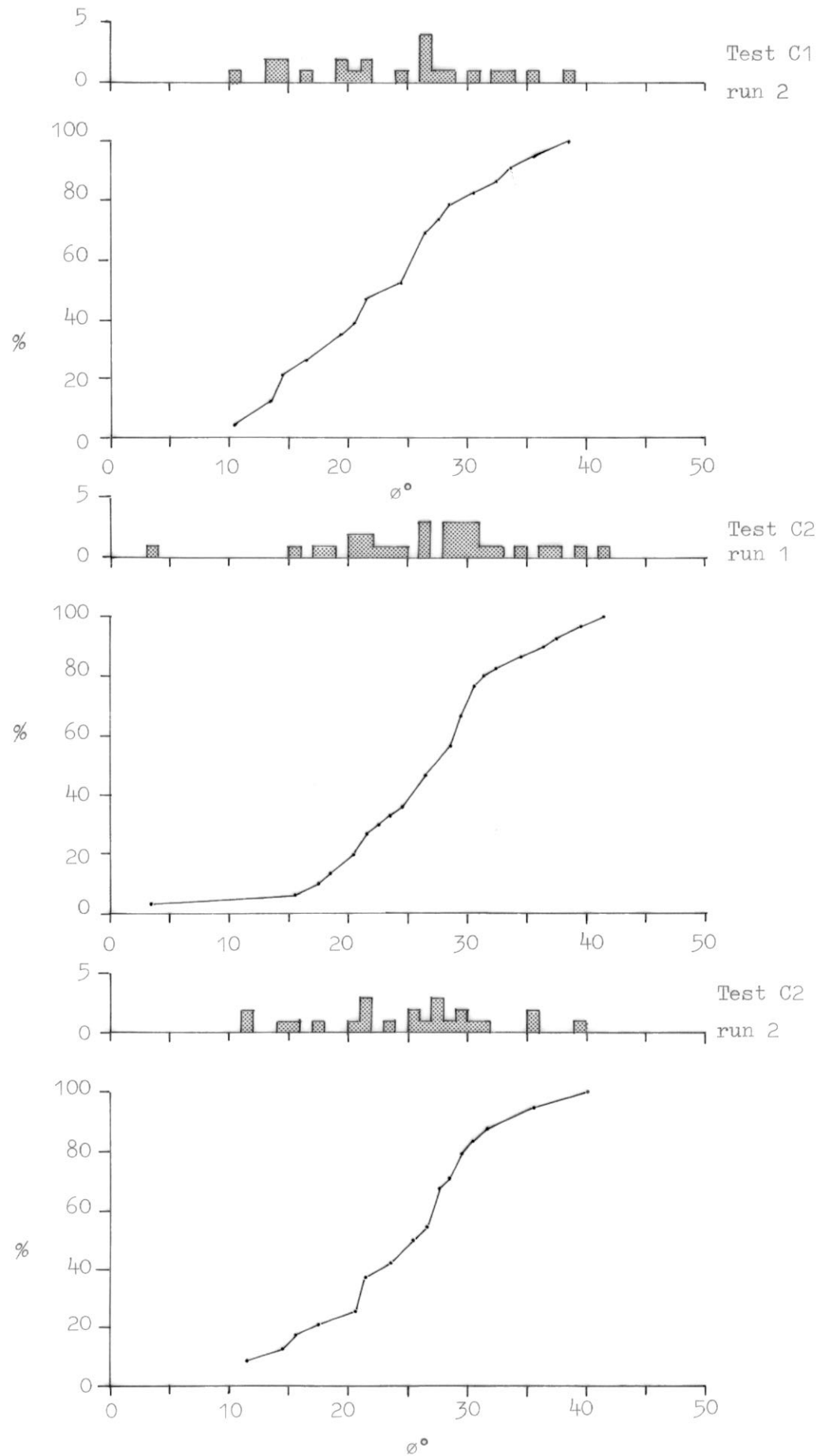


Figure 7.12. Scatter histograms and cumulative frequency graphs for ϕ° . Tests C1 run 2, C2 runs 1 & 2.

Darleydale Sandstone $\beta = 25^\circ$

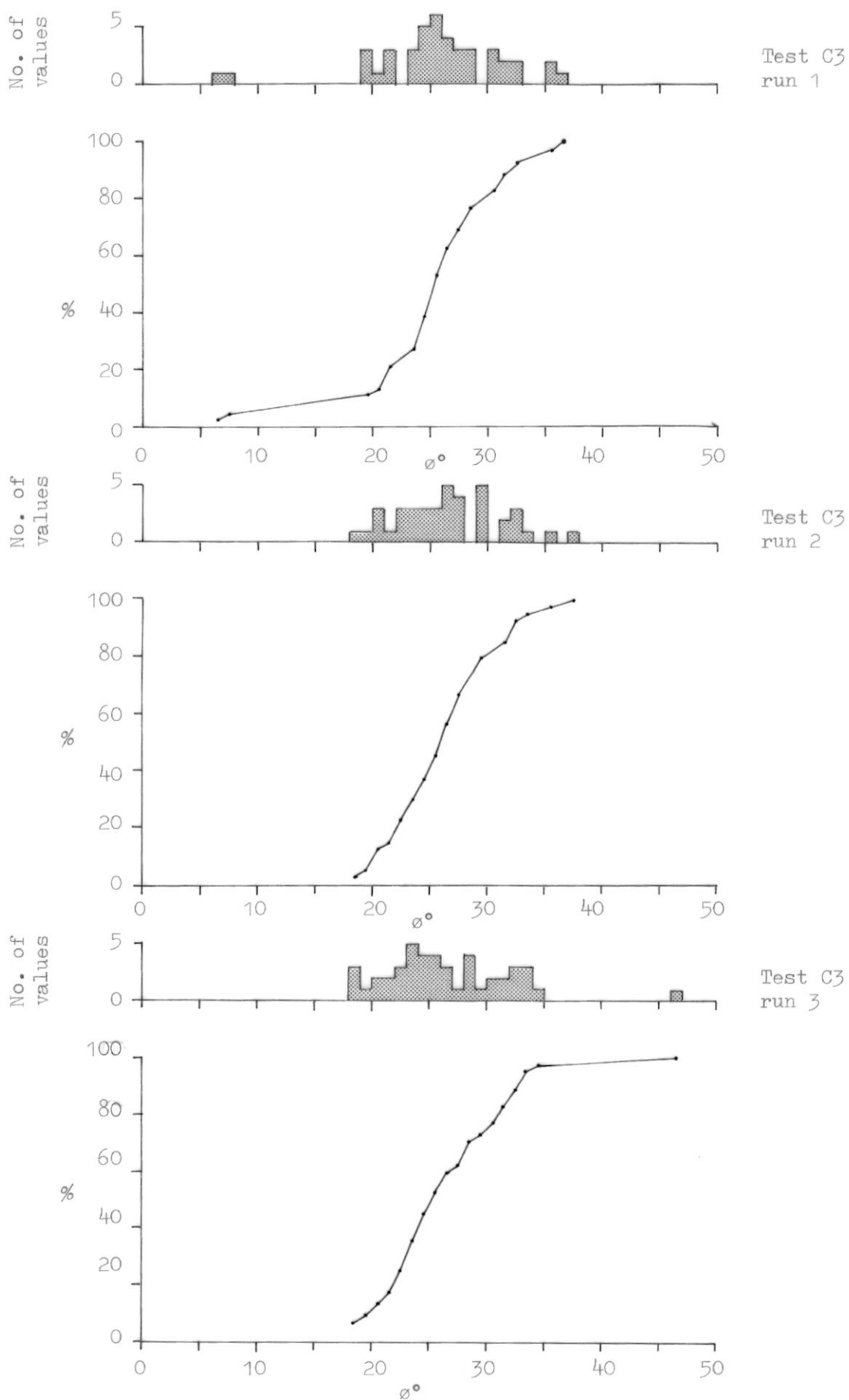


Figure 7.13

Scatter histograms and cumulative frequency graphs for ϕ° .
 Test C3, runs 1 2 and 3.
 Darleydale Sandstone $\beta = 20^\circ$

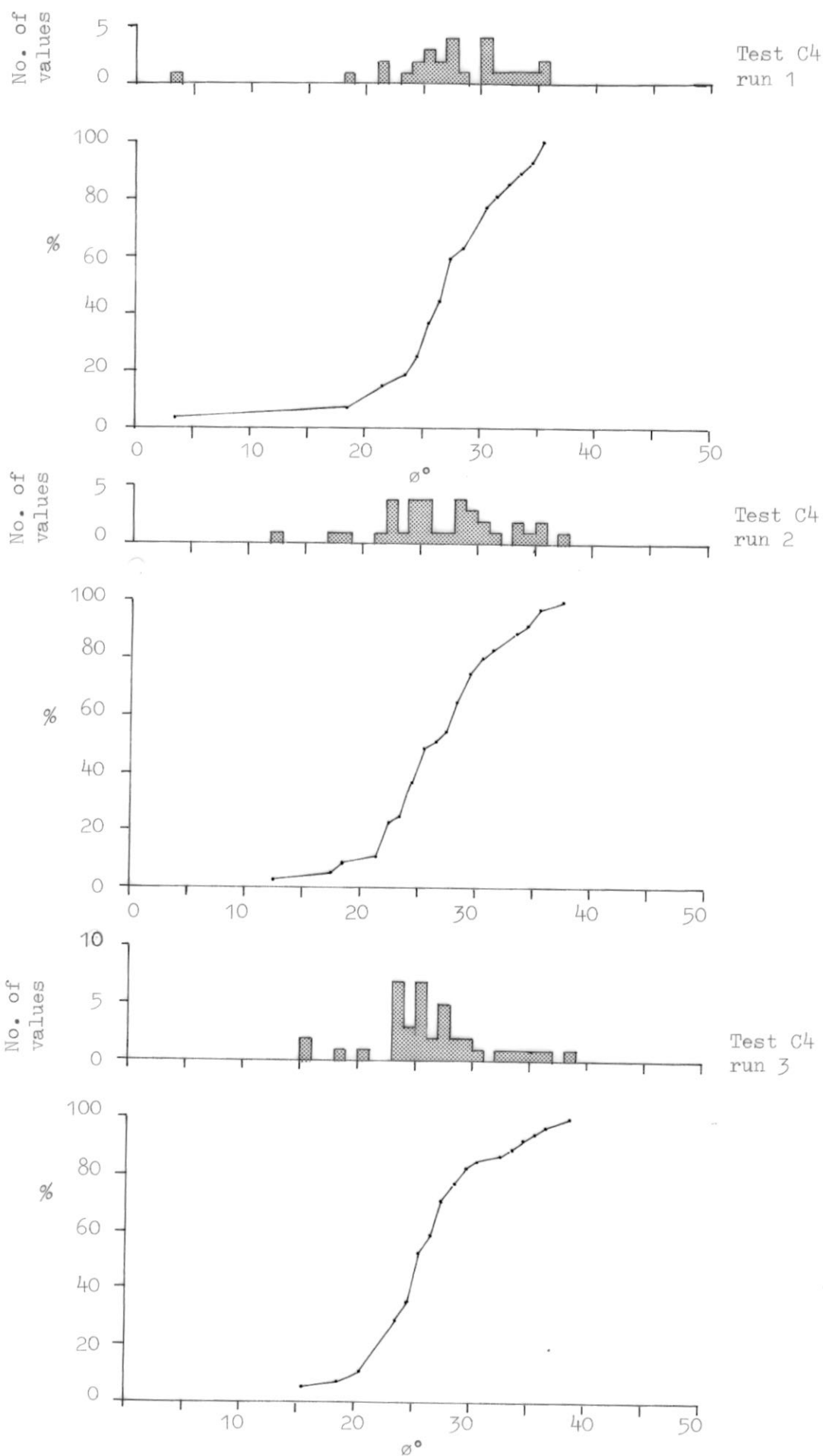


Figure 7.14 Scatter histograms and cumulative frequency graphs for ϕ° .
 Test C4, runs 1 2 and 3.
 Darleydale Sandstone $\beta = 20^\circ$.

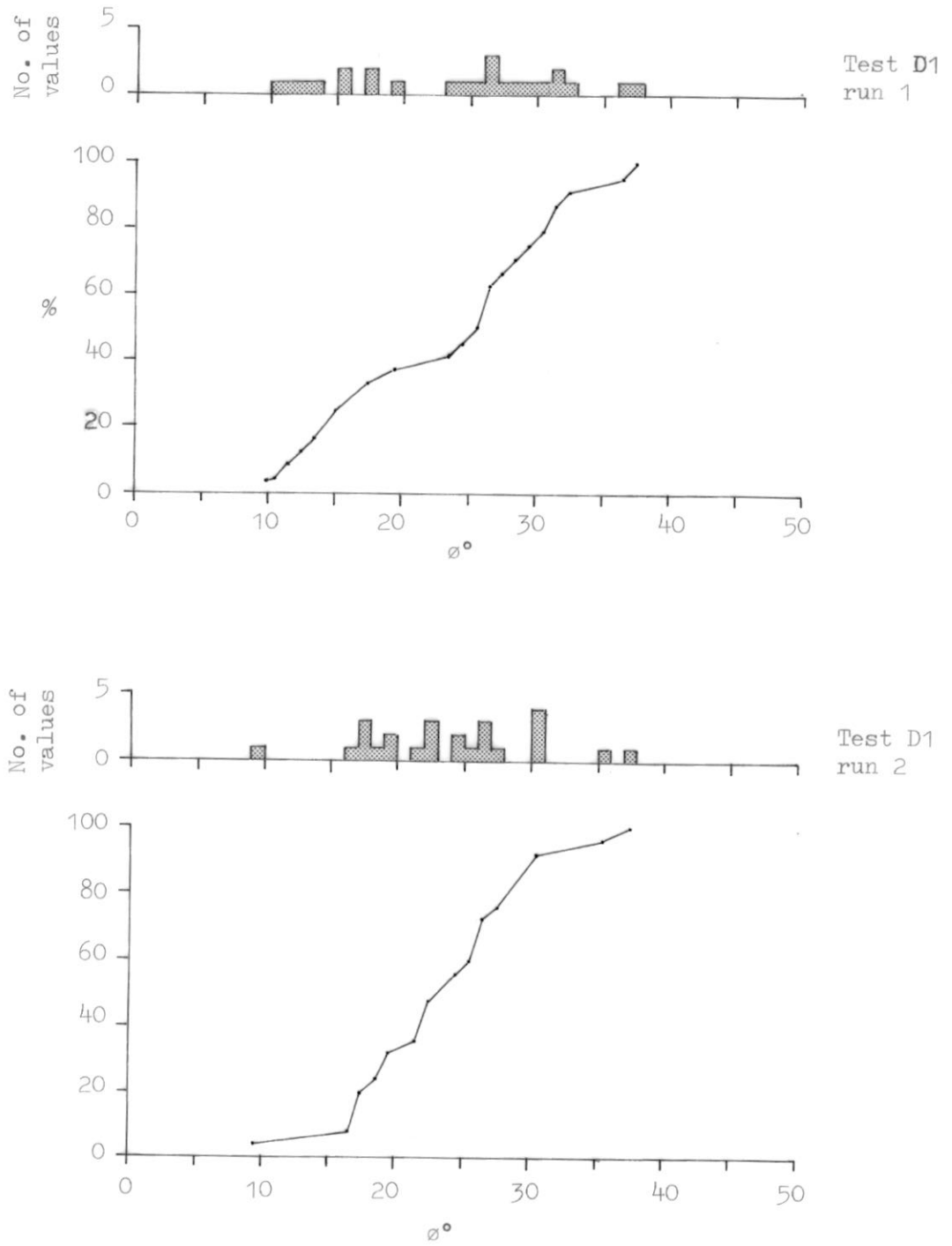


Figure 7.15 Scatter histograms and cumulative frequency graphs for ϕ° .
 Test D1, runs 1 and 2.
 Permian Sandstone $\beta = 25^\circ$

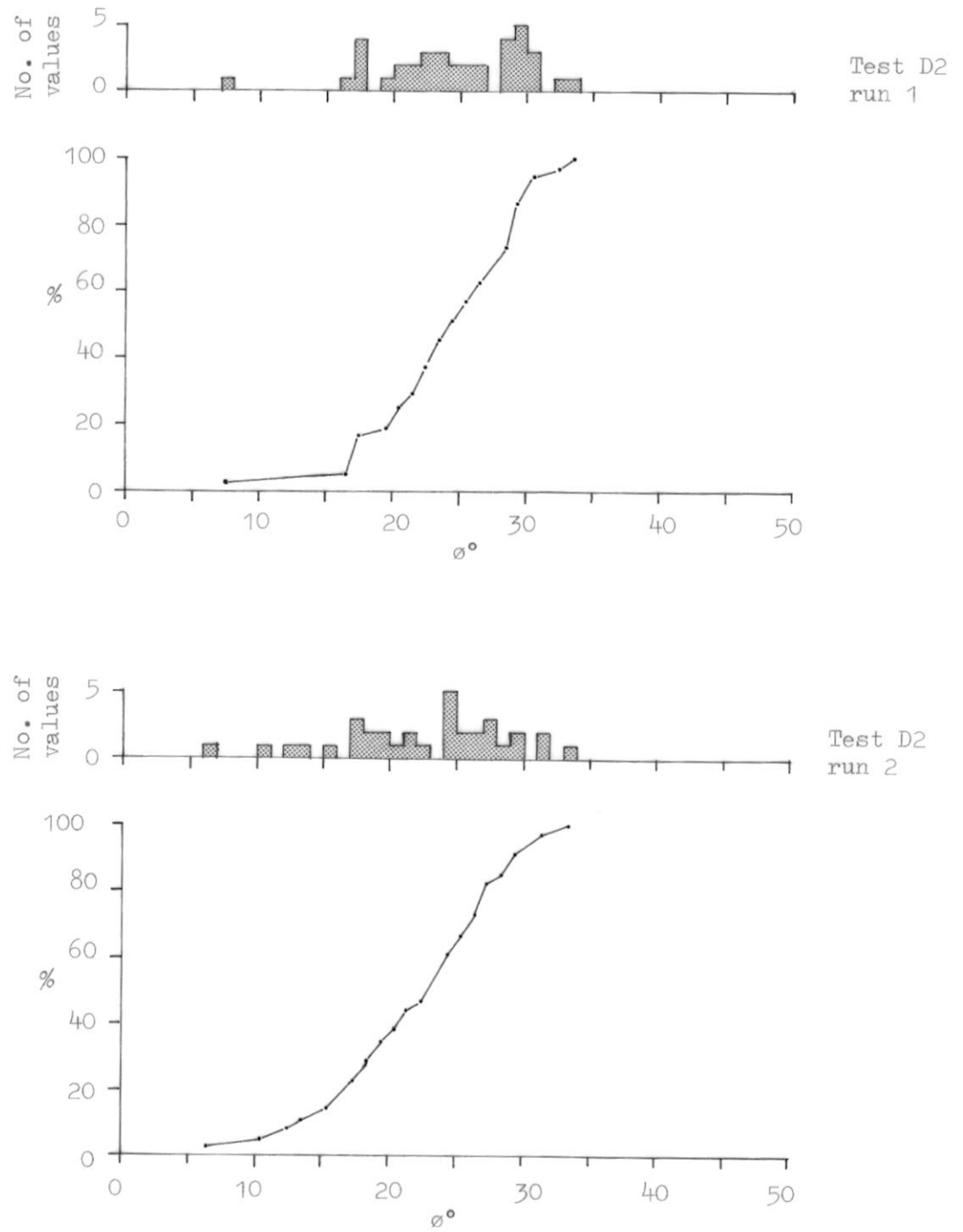


Figure 7.16 Scatter histograms and cumulative frequency graphs for ϕ°
 Test D2. runs 1 and 2
 Permian Sandstone $\beta = 20^\circ$

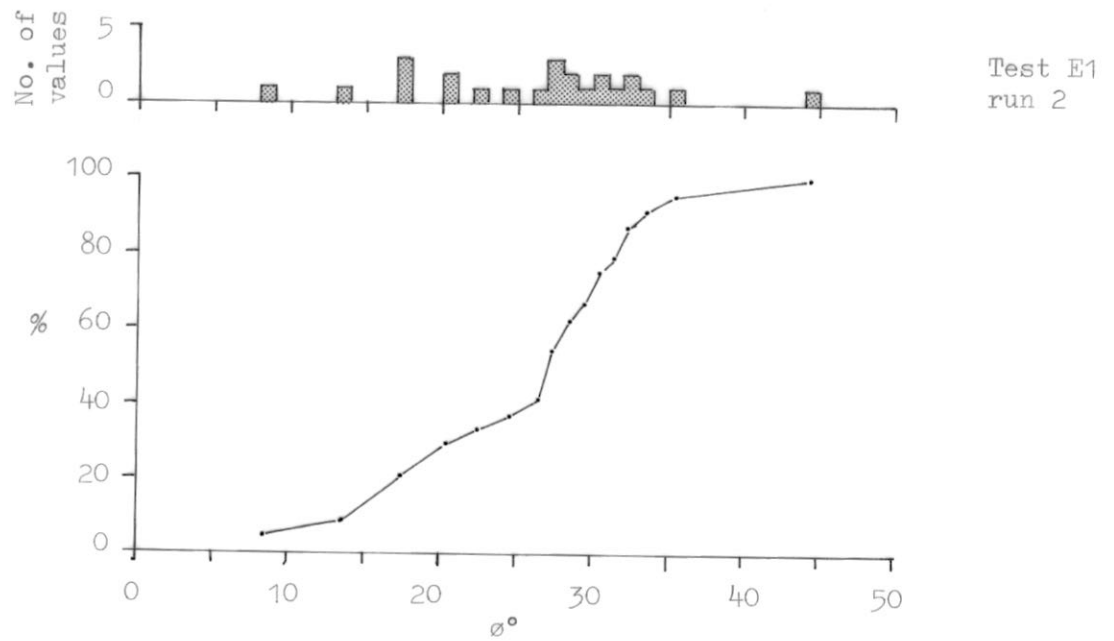
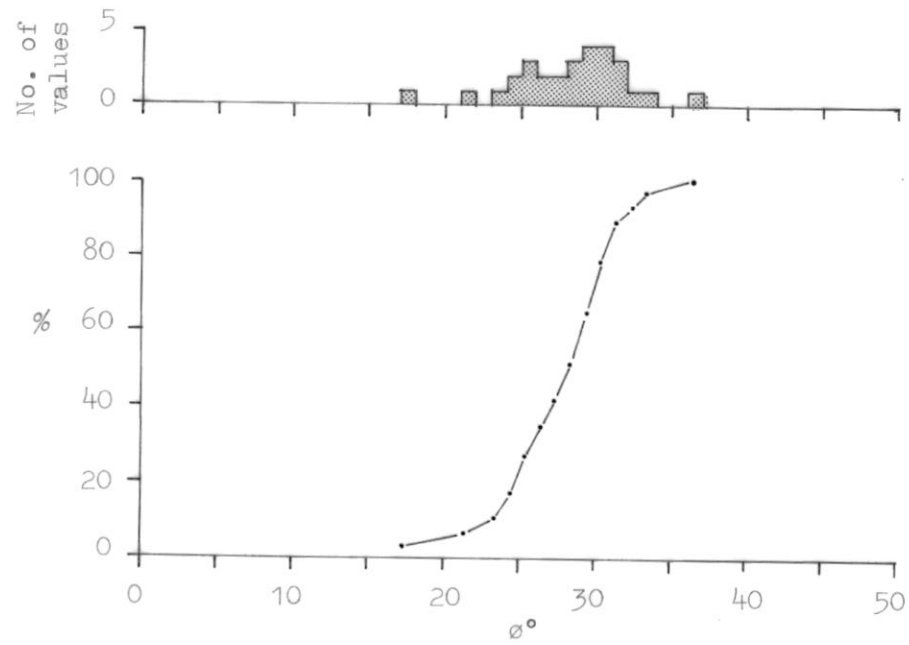


Figure 7.17 Scatter histograms and cumulative frequency graphs for ϕ° .
Test E1, runs 1 and 2.
Delabole Slate $\beta = 25^\circ$

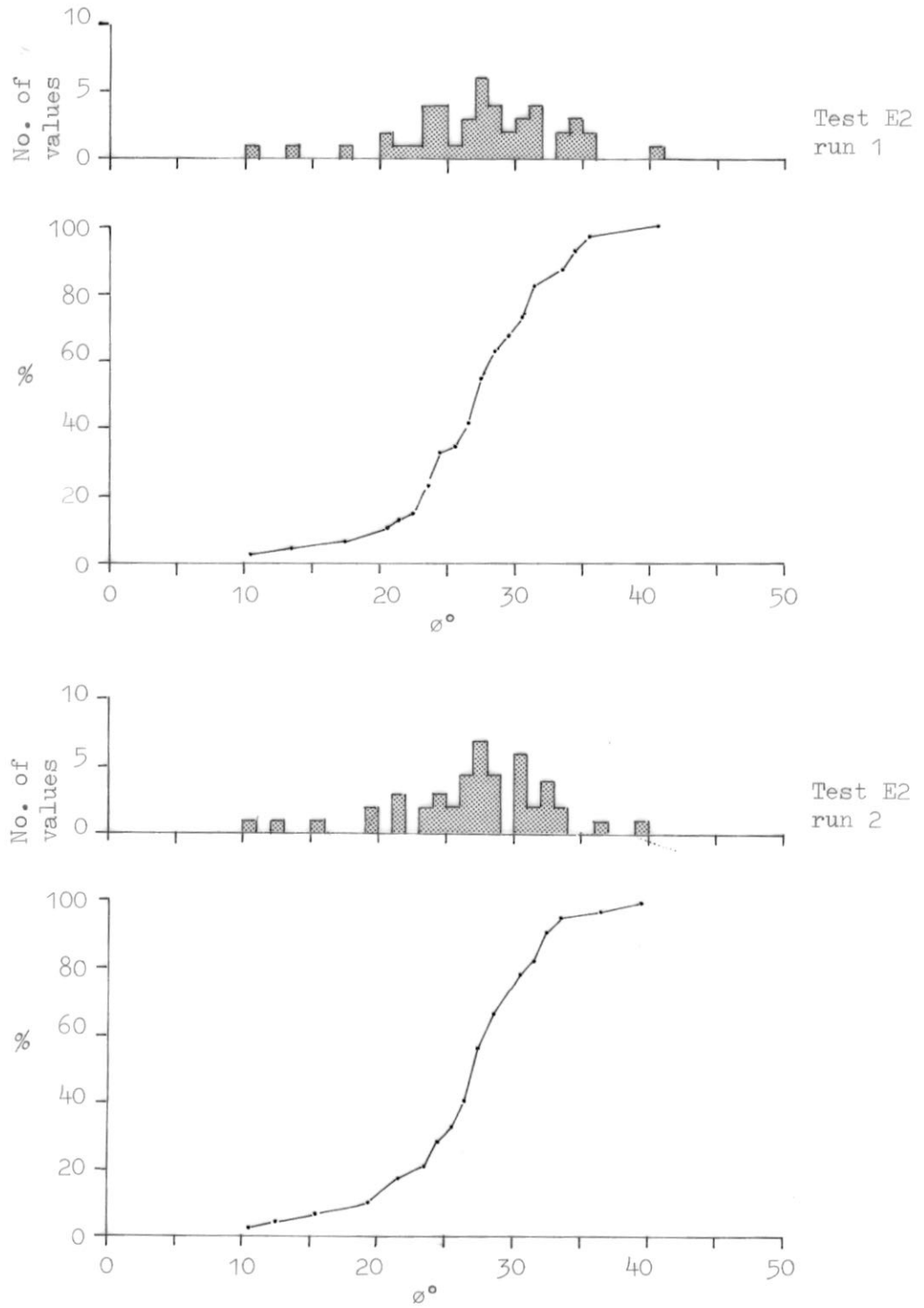


Figure 7.18 Scatter histograms and cumulative frequency graphs for ϕ° .
 Test E2, runs 1 and 2.
 Delabole Slate $\beta = 20^\circ$.

Results from all tests using Darleydale Sandstone, Permian Sandstone and Delabole Slate are compared in figure 7.19 with results from inclined plane sliding tests.

In the case of Darleydale Sandstone results from two inclined plane sliding tests are given (blocks M4 and M5).

Several facts are apparent from this figure :

- i) In all cases ϕ_m is less than ϕ_{av} .
- ii) For all rock types but especially for Permian Sandstone and Portland Limestone (figures 7.10 and 7.11) peak angles of sliding from inclined plane sliding tests are higher than ϕ_m for equivalent displacements.
- iii) For Delabole Slate, peak sliding angles are very close to ϕ_{av} .

The difference between ϕ_m and ϕ_{av}

The values for ϕ_m and ϕ_{av} are both obtained from the same test results. ϕ_m is calculated from incremental displacements of the block; ϕ_{av} is determined by calculating the equivalent constant angle of friction that would result in the same total displacements from the same input force history.

In all tests it has been seen that ϕ_{av} is greater than ϕ_m by up to 5° . If ϕ_m was a constant for a whole run then the displacements resulting would be greater than if ϕ_{av} represented the friction angle. This discrepancy is explained in the following way. In these vibration tests incremental values for ϕ , (from which ϕ_m is determined), are only obtained for times at which the block is actually moving. It is proposed therefore, that during vibration test runs there were periods during which the block was stationary even though the ratio of shear load to

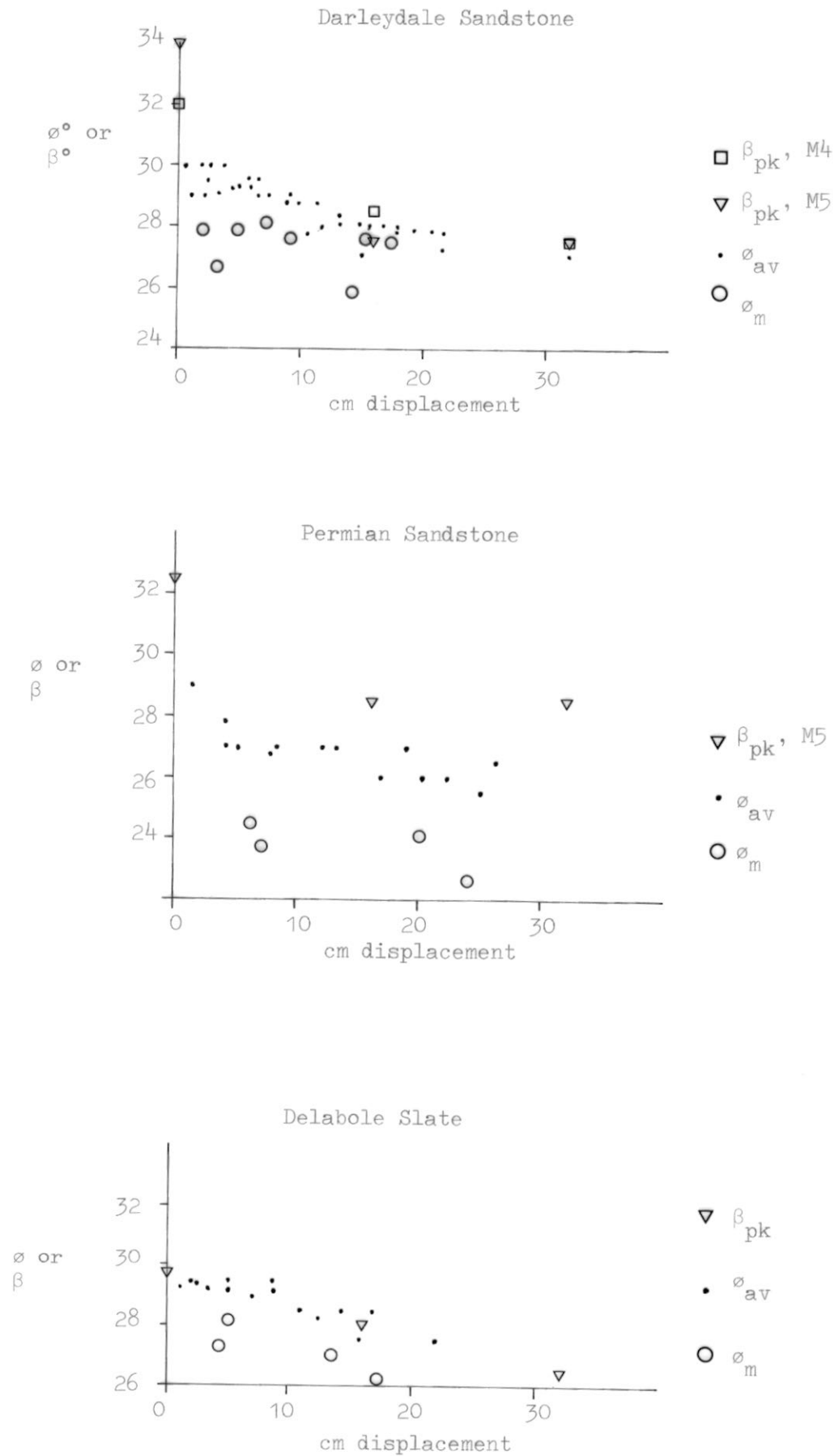


Figure 7.19 Comparison of peak sliding angles (β°) from inclined plane sliding tests to angles of friction from vibration tests, against displacement.

normal load was greater than $\tan \phi_m$, these periods being followed by periods of movement in which the operative angle of friction was ϕ_m . The displacement of the block in a given time would be less than that predicted if ϕ_m governed both the strength before the block began moving as well as when moving.

This is illustrated diagrammatically in figure 7.20.

The calculated mean value for friction whilst the block was moving was ϕ_m . Therefore, the block should have begun sliding at time t_1 when $S = N \tan \phi_m$, ($\ddot{x}_s = \ddot{x}_n \tan \phi_m$) where $S = m \cdot \ddot{x}_s$ and $N = m \cdot \ddot{x}_n$.

The block should have stopped moving at t_6 so that

$$\int_{t_1}^{t_6} \ddot{x}_s - \ddot{x}_n \cdot \tan \phi_m \cdot dt = 0 \quad (\text{Velocity})$$

The total displacement of the block during this cycle of movement is given by

$$\iint_{t_1}^{t_6} \ddot{x}_s - \ddot{x}_n \cdot \tan \phi_m \cdot dt \cdot dt = D(\phi_m)$$

However the true displacement in this time was $D(\phi_{av})$ which was less than $D(\phi_m)$ and gave an equivalent constant angle of friction during sliding of ϕ_{av} , higher than ϕ_m . In figure 7.20 the double integration of $\ddot{x}_s - \ddot{x}_n \cdot \tan \phi_{av}$ between times t_2 and t_4 would give a displacement of $D(\phi_{av})$.

The operative angle of friction during sliding was, however, ϕ_m . The low value of displacement measured therefore, may be explained where the block did not actually begin moving until time t_3 when the operative angle of friction was ϕ_p . Once sliding was initiated the frictional resistance dropped so that the displacement measured

$$D_{(av)} = \iint_{t_3}^{t_5} \ddot{x}_s - \ddot{x}_n \tan \phi_m \cdot dt \cdot dt.$$

To prove this hypothesis it was necessary to re-examine the graphical output from EINSTET.

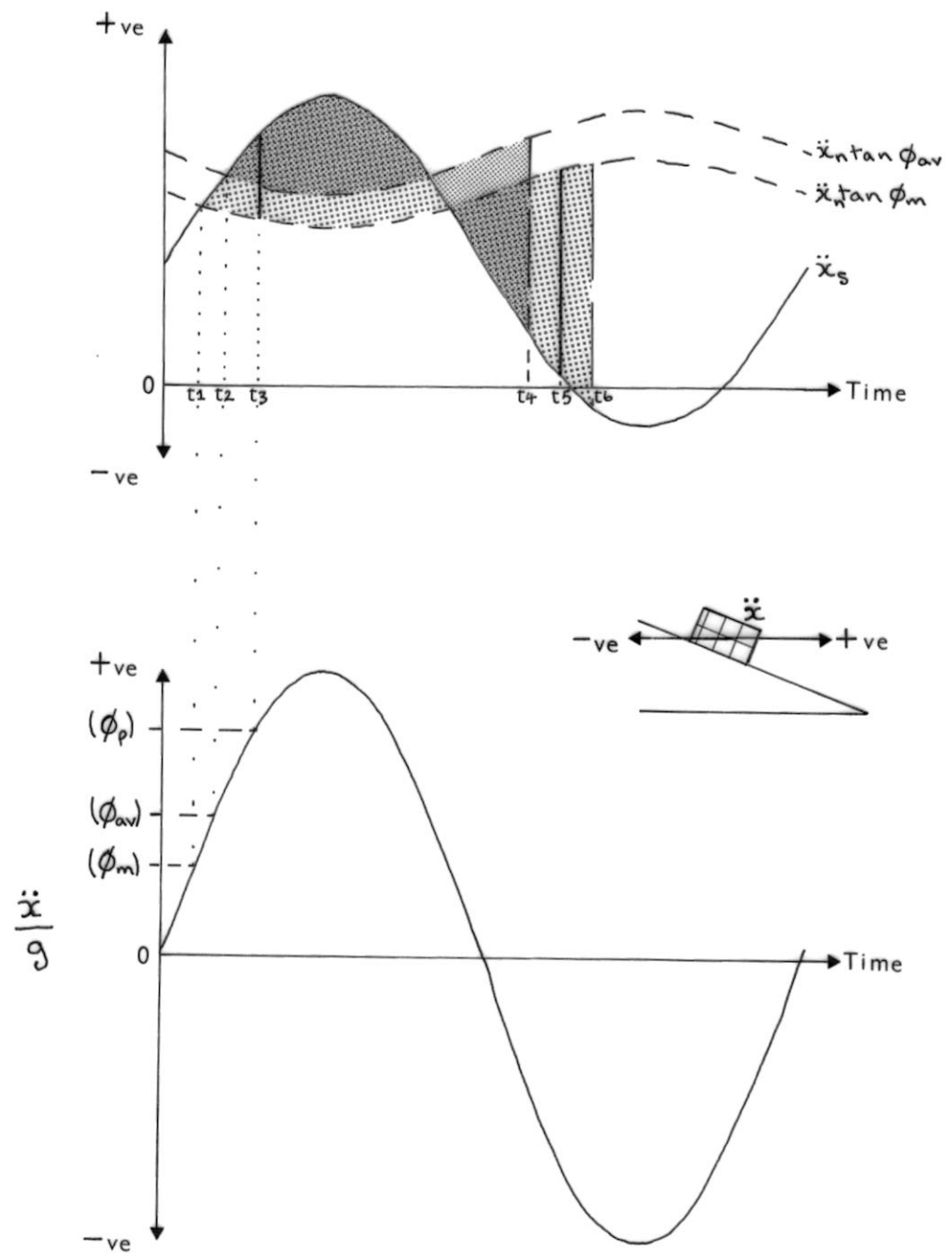


Figure 7.20 To explain the discrepancy between ϕ_m and ϕ_{av} in terms of a peak friction angle ϕ_p .

By extrapolating the graph giving displacement increments (DISP INC) it is possible to determine the time at which the block actually began moving (at the start of each cycle of movement). The horizontal acceleration acting at that time can be obtained from the graph (BASAL ACC). Using the equation

$$\frac{\ddot{x}_c}{g} = \tan (\phi - \beta) \quad (\text{see chapter 3})$$

values for ϕ_p are obtained for the onset of sliding. Alternatively the graph (SHEAR COEF) can provide the value of shear coefficient (S/N) at the relevant time. Table 7.4 has been drawn up from data obtained in this way.

Values for ϕ_p were found to be much higher than the calculated value of ϕ_m or ϕ_{av} . These peak values occurred at the beginning of each cycle of movement and therefore several values for ϕ_p were obtained for each test run. It was found that the value of ϕ_p generally decreased during each test run and it is this range of values that are given in table 7.4. These results and their significance are discussed in detail in the following section.

The physical meaning of ϕ_p and ϕ_m

Peak Values (ϕ_p)

Several conclusions may be drawn from the data given in table 7.4.

- 1) ϕ_p is higher than ϕ_m or ϕ_{av} as would be necessary to explain the discrepancy between ϕ_m and ϕ_{av} .
- 2) Values for ϕ_p for early displacement cycles in each run are much higher than the equivalent peak angles of sliding obtained from inclined plane tests.
- 3) ϕ_p decreases during each run.
- 4) ϕ_p for the same rock type decreases with decreasing angle of slope (β°).

TEST NO.	RUN NO.	RANGE OF VALUES FOR ϕ_p	β°	Equivalent Inclined Plane Sliding angle - (start of run)
B4	1	51 to 48	30	38
	2	51 to 47	30	35.5
	3	46	25	34.5
	4	41 to 40	20	32.5
	5	33 to 32	15	30
	6	32 to 28	10	28
	7	31 to 28	10	25
	8	30 to 27	10	22
	9	31 to 29	10	20
	10	32 to 28	10	19
	11	28	10	19
	12	30 to 28	10	19.5
	13	29 to 28	10	20
	14	29	10	19
	15	30 to 27	10	18.5
	16	30 to 27	10	19
	17	30 to 28	10	20.5
C1	2	41	25	28
C2	1	44 to 41	25	33
	2	43 to 42	25	28
C3	1	38 to 30	20	33
	2	38 to 32	20	28
	3	38 to 29	20	27.5
C4	1	39 to 33	20	33
	2	39 to 33	20	28
	3	39 to 33	20	27.5
C5	1	40 to 34	22.5	33
	2	44 to 37	22.5	28
D1	1	44 to 39	25	32.5
	2	44 to 43	25	28.5
D2	1	40 to 33	20	32.5
	2	40 to 33	20	28.5
E1	1	43 to 40	25	29.75
	2	44 to 42	25	28
E2	1	38 to 32	20	29.75
	2	38 to 32	20	28

Table 7.4 Range of values for ϕ_p from tests B4, C1, C2, C3, C4, C5, D1, D2, E1, E2.

To investigate these conclusions in more detail consider the results from tests using Permian Sandstone, (tests D1 and D2). Values for ϕ_p are obtained from the graphs given in figures 7.21 to 7.24. Extrapolation of the displacement increment graphs give the approximate times for commencement of sliding. Values for the horizontal accelerations (\ddot{x}_c) acting at these times are given in table 7.5. Also given in this table are the calculated values of ϕ_p for the initiation of each displacement cycle. The important variations in ϕ_p both with angle of slope and within each run are evident from this data. Considering the second point it is clear that the decrease in ϕ_p during each run is not due to wear of the surfaces as the results from D2 run 2 are almost identical to those for run 1, even though run 2 was carried out using the same surfaces as in run 1.

The common variable factor in all tests is the rate of loading. In section 7.3 it was proposed that a lag in the response of surfaces to impulse loading might result in delayed sliding. In these vibration tests two interrelated processes are involved as the inertia force, directed out of the inclined plane, increases:

- i) The normal load is decreased resulting in a reduced area of contact and reduced interlocking and hence a reduced strength.
- ii) Adhesional bonds and interlocked grains are acted upon by increasing shearing forces.

If these reactions to the changing components of load are not instantaneous then the measured strength of the surfaces will be higher than if the reactions were in phase with the applied loads. It is suggested that the reactions are not instantaneous and the measured peak strengths are therefore dependant upon the rate of change of the applied loads.

A relationship was therefore sought between the rate of change of load and the peak sliding resistance of the block that would explain

TEST NO.	DISPLACEMENT CYCLE (see figs.)	\ddot{x}_c	\ddot{x}_1	\ddot{x}_2	ϕ_p°
		cm.sec ⁻²			
D1 Run 1 $\beta = 25^\circ$	1	-336	371	-359	43.9
	2	-321	348	-336	43.1
	3	-249	324	-313	39.2
D1 Run 2 $\beta = 25^\circ$	1	-328	374	-359	43.5
	2	-275	351	-336	40.7
	3	-311	325	-315	42.6
D2 Run 1 $\beta = 20^\circ$	1	-357	371	-357	40
	2	-331	351	-331	38.7
	3	-298	325	-310	36.9
	4	-275	305	-290	35.7
	5	-270	282	-270	35.4
	6	-240	263	-249	33.7
	7	-232	244	-232	33.3
D2 Run 2 $\beta = 20^\circ$	1	-359	371	-359	40
	2	-334	351	-334	38.8
	3	-296	321	-309	36.8
	4	-273	301	-290	35.6
	5	-230	282	-268	33.2

Table 7.5 Reduction in ϕ_p with rate of change of normal component of acceleration.

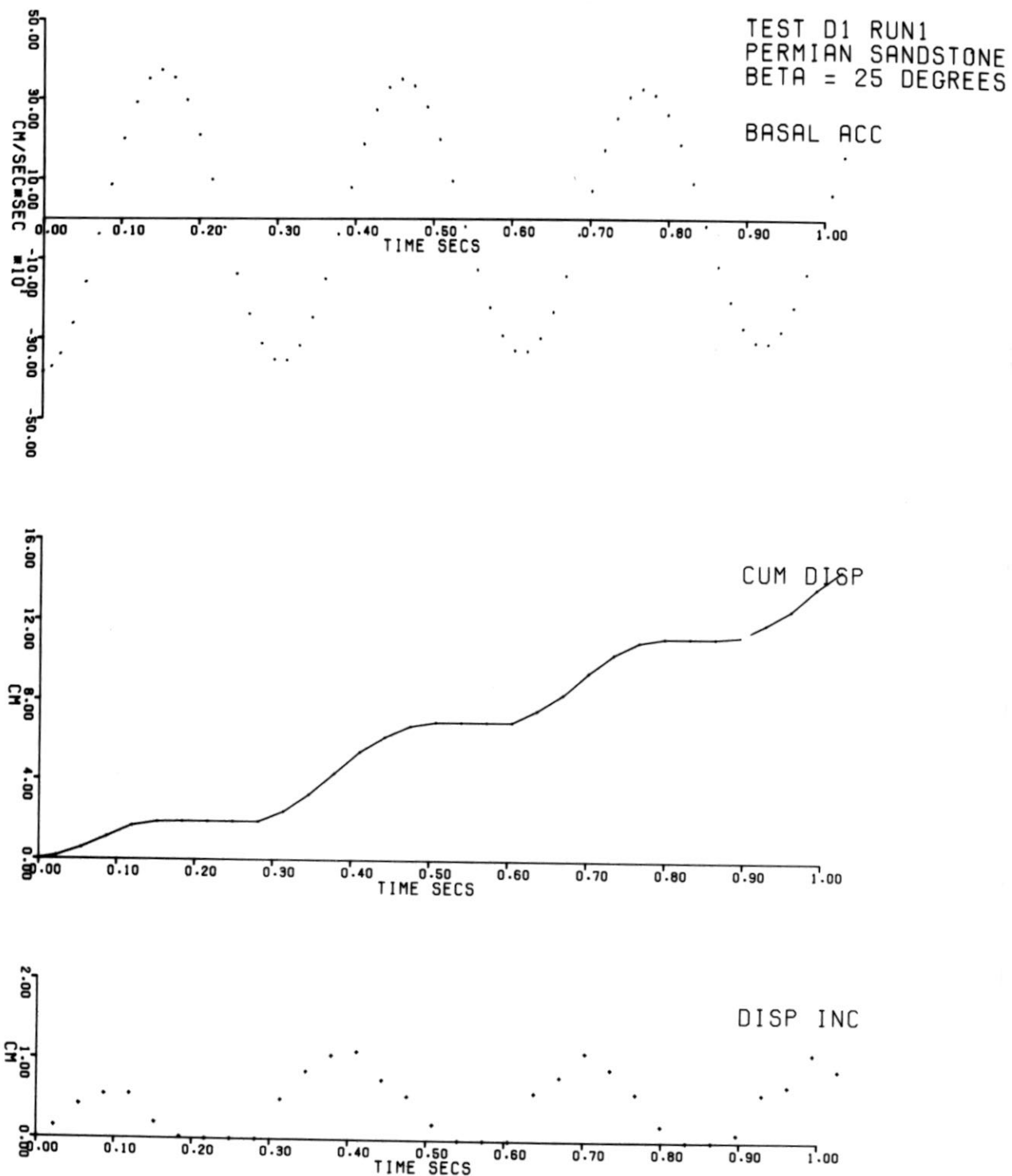


Figure 7.21

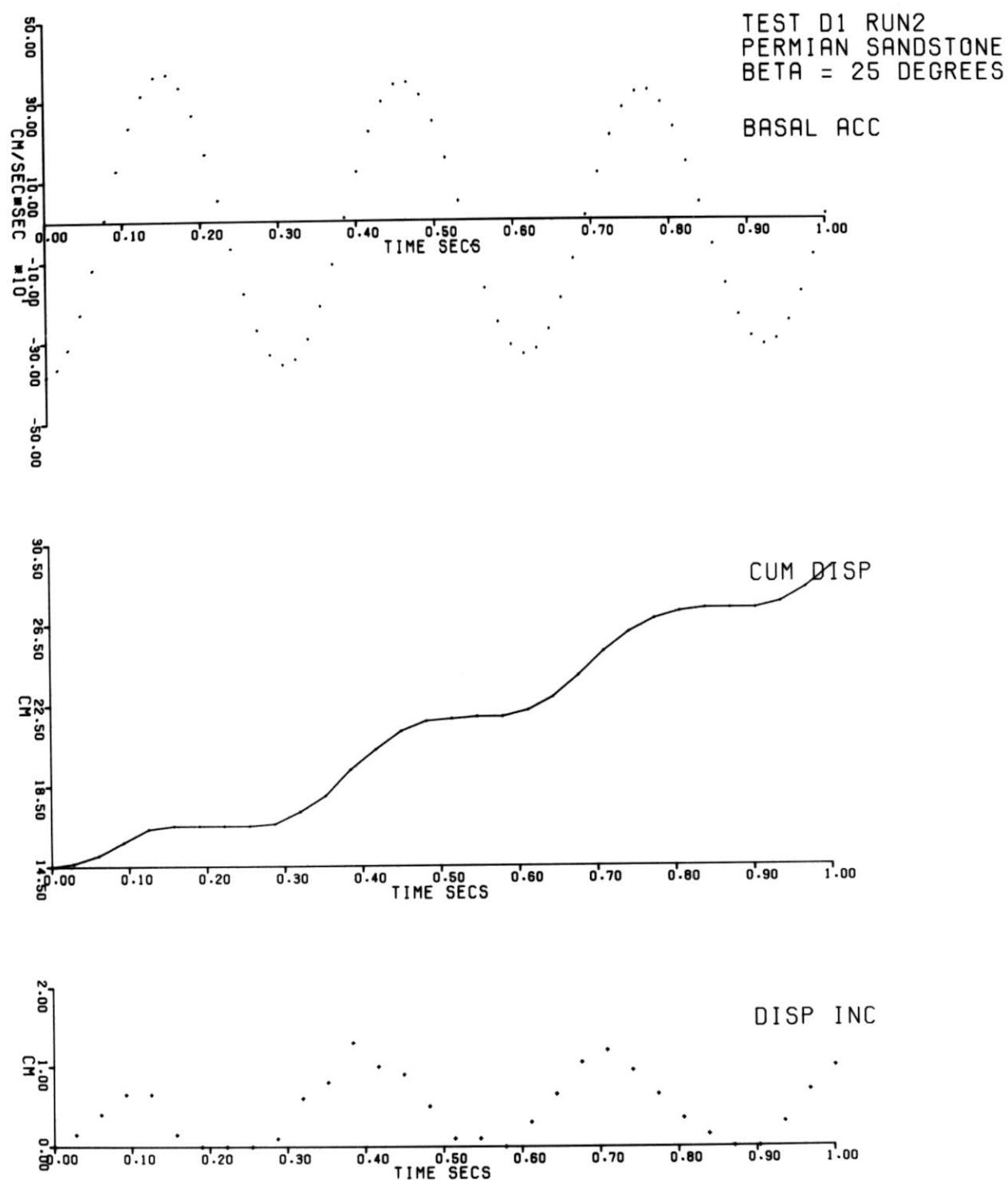


Figure 7.22

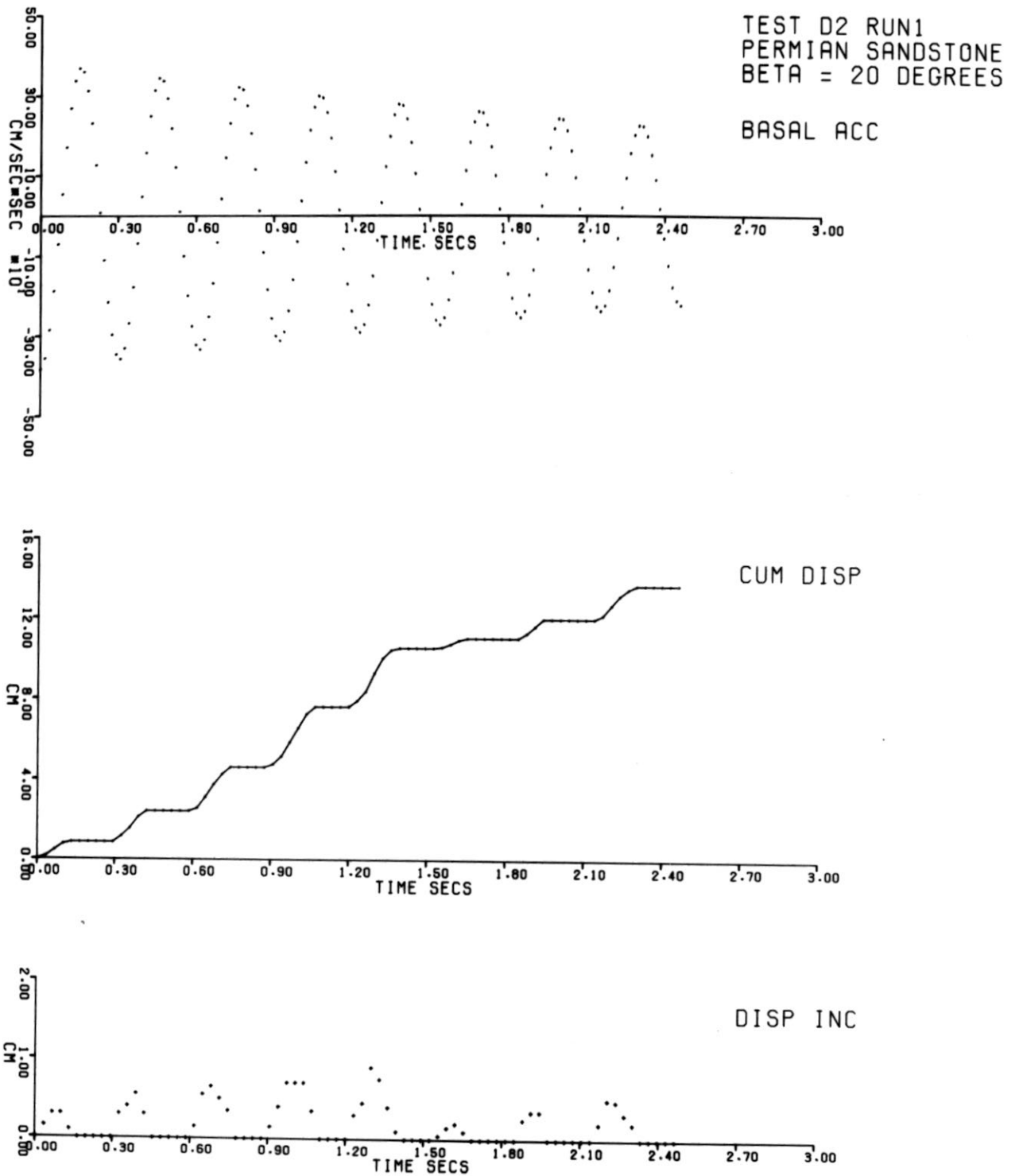


Figure 7.23

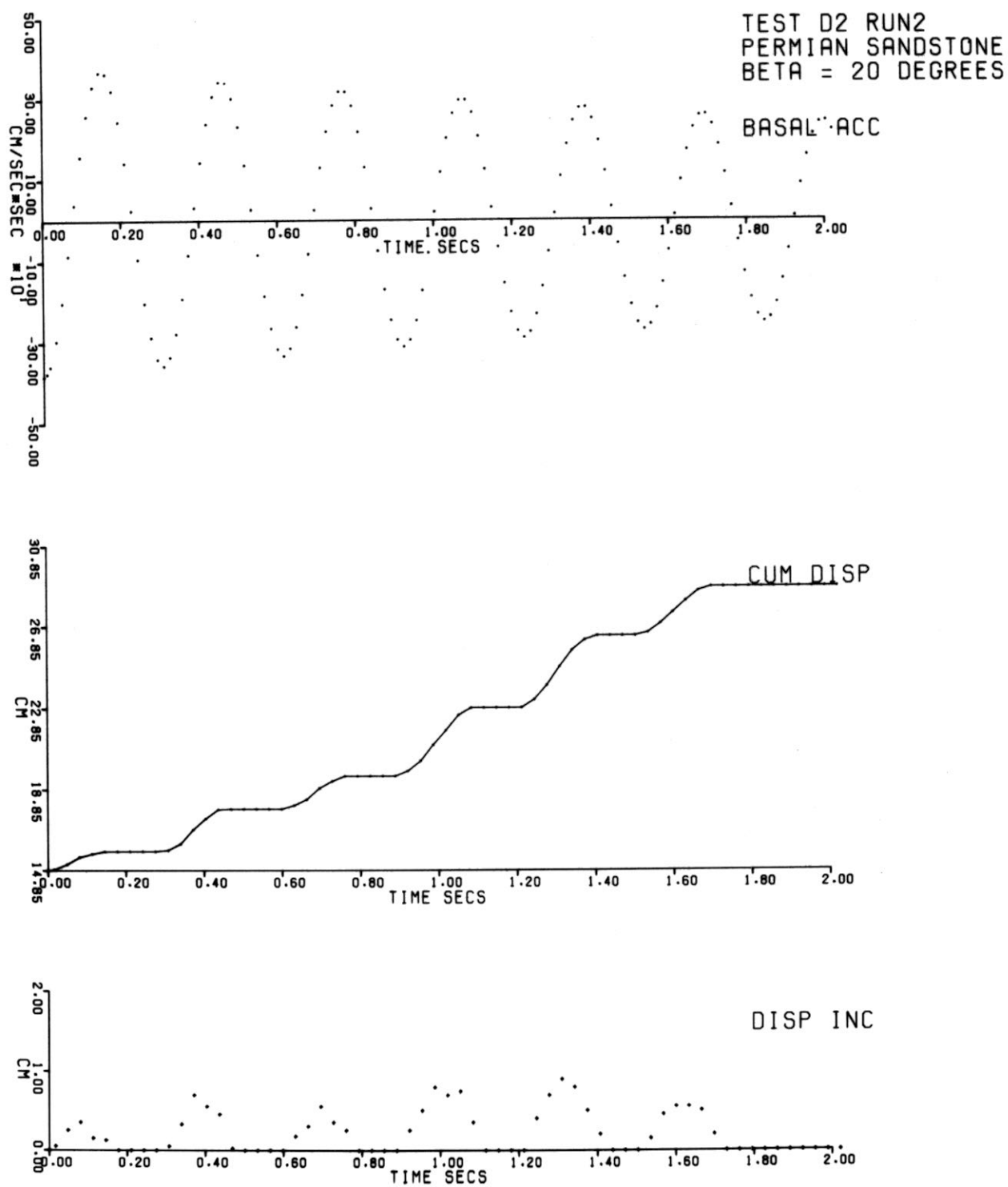


Figure 7.24

both the decrease in ϕ_p with angle of slope and decrease in ϕ_p during an individual run. Clearly, for a given block and basal acceleration-time record, the total inertial and gravitational forces acting on the block do not vary with angle of slope: the variation of ϕ_p with angle of slope cannot be explained by considering the rate of change of total forces. Components of shear load and normal load do vary both with angle of slope and with the amplitude of applied acceleration.

Consider the general case of a block on an inclined plane where a horizontal simple harmonic acceleration is applied. Let $|\ddot{x}_p|$ be the magnitude of the peak horizontal acceleration, repeated after $\frac{T}{2}$ secs where T is the period of motion. From the analysis of a block on an inclined plane (chapter 3) it is clear that the shear load will vary between

$$m.g.\sin \beta + m.\ddot{x}_p.\cos \beta \quad \text{and} \quad m.g.\sin \beta - m.\ddot{x}_p.\cos \beta$$

in time $\frac{T}{2}$.

The normal load will vary between

$$m.g.\cos \beta - m.\ddot{x}_p.\sin \beta \quad \text{and} \quad m.g.\cos \beta + m.\ddot{x}_p.\sin \beta \quad \text{in the same time.}$$

It has been indicated that the reaction to both applied normal and shear loads will be important to measured strength and it is necessary therefore to consider both components combined in order to explain the peak values obtained. By rearranging the equations given above it is found that the ratio of shear load to normal load, (S/N) , varies between

$$\frac{\tan \beta + \ddot{x}/g}{1 - \frac{\ddot{x}}{g} \tan \beta} \quad \text{and} \quad \frac{\tan \beta - \ddot{x}/g}{1 + \frac{\ddot{x}}{g} \tan \beta}$$

in time $\frac{T}{2}$ secs.

In figure 7.25 the maximum and minimum values for this shear coefficient are given for various slope angles and horizontal peak accelerations.

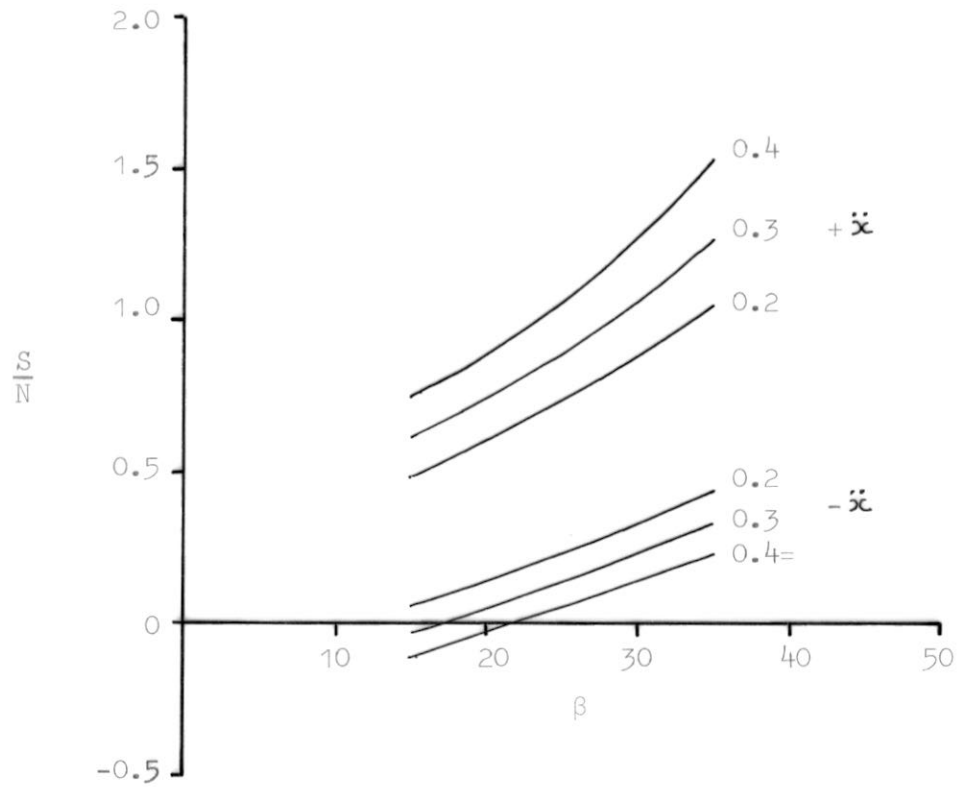


Figure 7.25 Maximum and minimum values of S/N for various slope angles and applied horizontal accelerations.

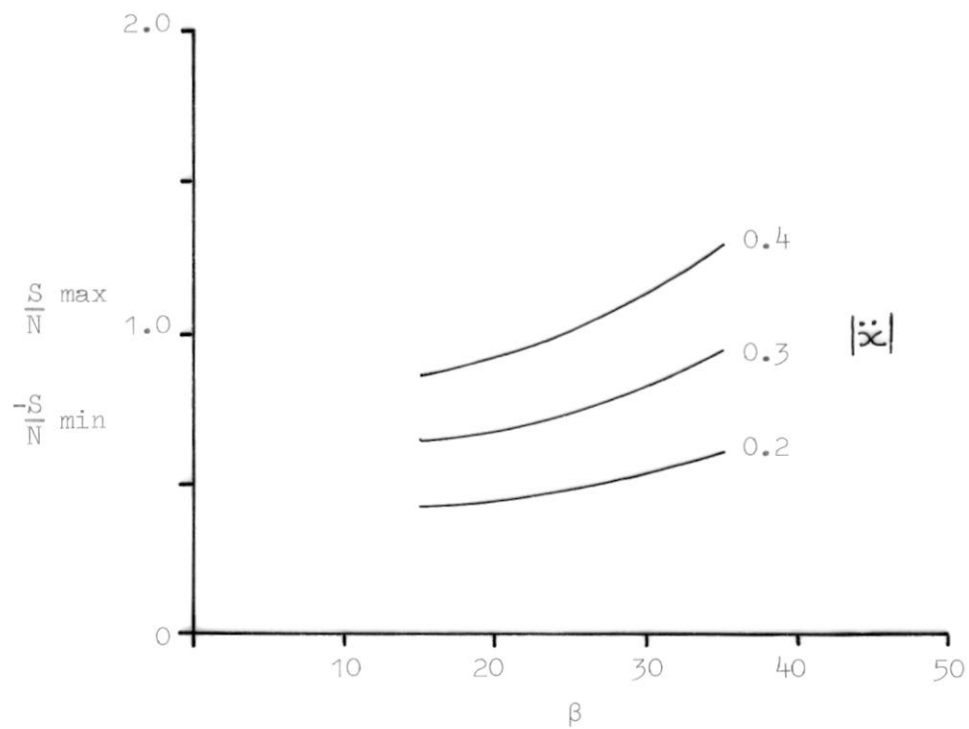


Figure 7.26 Difference between maximum and minimum values of S/N for various slope angles and applied horizontal accelerations.

In figure 7.26 the total change in shear coefficient is given for the same slope angles and peak accelerations. Taking the period of the horizontal acceleration to be a constant (as it was in the vibration tests considered here) the following conclusions may be drawn:

- 1) For the same horizontal acceleration, the rate of change of shear coefficient $\frac{\Delta S/N}{T/2} = \frac{2 \cdot \Delta S/N}{T}$ decreases with decreasing angle of slope.
- ii) For the same angle of slope, the rate of change of shear coefficient decreases with decreasing horizontal acceleration [as in the damped harmonic motion applied in these tests].

These are exactly the results required if it were to be shown that measured values of ϕ_p were dependant upon the rate of change of applied loads.

Considering the test data, maximum and minimum values for $\frac{S}{N}$ were obtained by calculation using the peak values for acceleration preceding and following each value of ϕ_p (\ddot{x}_1 and \ddot{x}_2 in table 7.5). The rate of change was obtained by dividing the difference in these values by the time period between them (a constant for these tests).

In figure 7.27 peak values $\frac{S}{N}$ at sliding ($= \tan \phi_p$) are plotted against the calculated rates of change of shear coefficient. A clear relationship is shown to exist between these parameters. The data points fall fairly precisely on a curved line indicating that the increase in apparent shear strength is greater proportionally for high rates of change of shear coefficient than for low rates.

The implication of these results is that for higher frequency vibrations (higher rate of change) the critical acceleration to initiate sliding in a slope of a given angle will be higher than for low frequency vibrations.

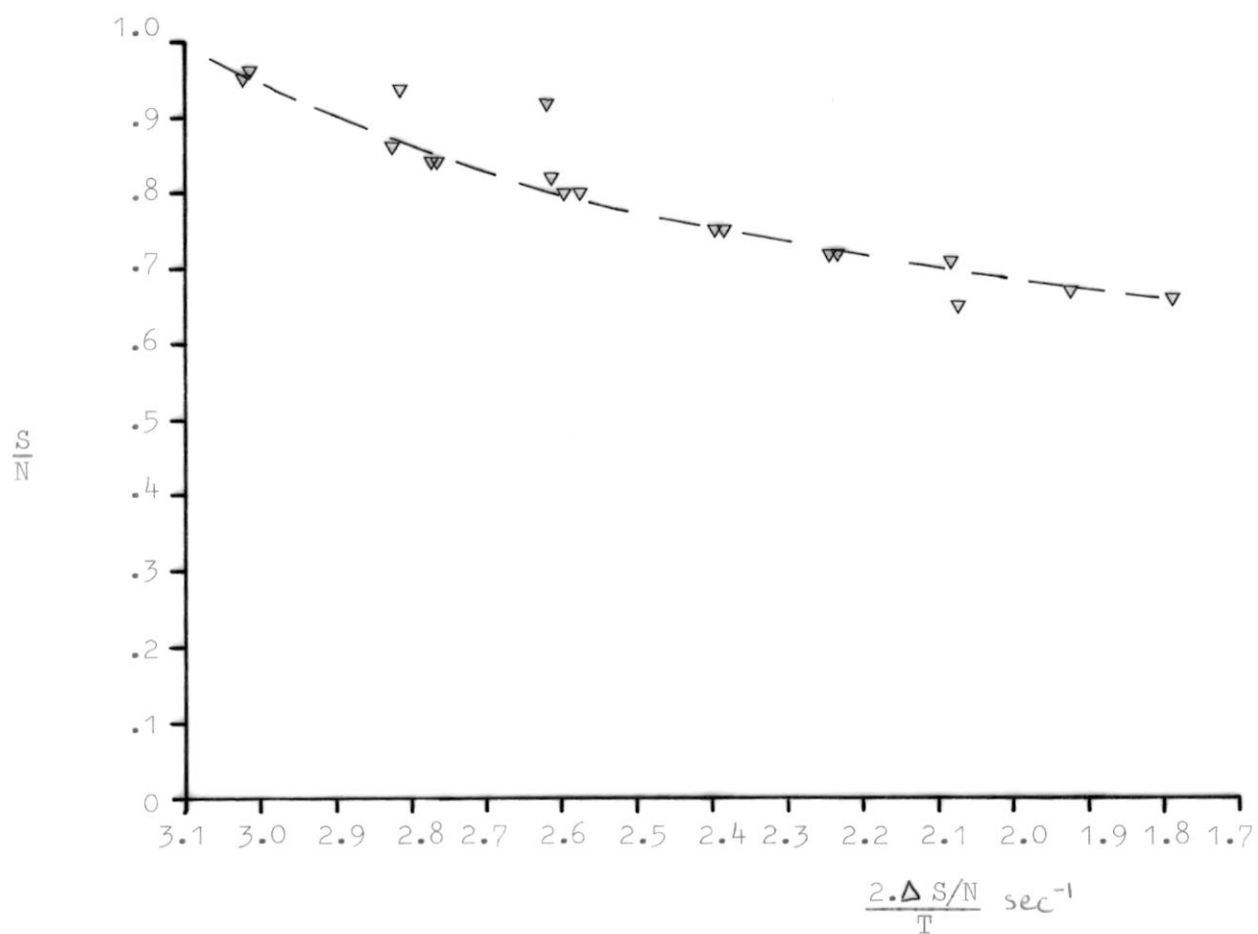


Figure 7.27 Relationship between measured values of S/N at the initiation of sliding and the rate of change of the ratio S/N

(Permian Sandstone)

S = Shear load

N = Normal load

T = Period of applied acceleration

Considering the fact that in these tests the block began sliding only when the applied horizontal acceleration approached its peak value it may be proposed that if the same acceleration had been applied but the frequency doubled (from 3 to 6 Hz), the block would not have been displaced at all. Further experimentation would be required to validate this.

It is proposed that the curve given in figure 7.27 will be asymptotic to the value of $\frac{S}{N}$ obtained from direct shear and inclined plane sliding tests where the rate of change of applied load ratio approaches zero. In the case illustrated the curve will be asymptotic to $\frac{S}{N} = 0.62$.

In no test using any rock type did the friction value for the initiation of sliding (ϕ_p) drop below the equivalent 'static' friction angle. In several tests, the block stopped sliding once the peak applied $\frac{S}{N}$ ratio dropped below the static friction coefficient for that rock type.

Mean values for ϕ (ϕ_m)

Once sliding, the frictional resistance between the rock surfaces is no longer a function of the rate of loading, being fairly constant for complete runs at different slope inclinations. Variation in values of ϕ_m for repeated runs can be related to decreasing frictional resistance with displacement (see figure 7.10).

For all rock types tested the mean values of sliding friction are less than the corresponding static angles of sliding obtained from inclined plane sliding tests. These low values are apparent immediately the rock begins sliding (even for fresh surfaces) and indicate different mechanisms controlling the frictional resistance for the static and sliding cases.

Consider in detail the results from Darleydale Sandstone tests C2 C3 and C4 (omitting C1 because the first run was not recorded successfully and C5 because of the large amount of scatter). Values for ϕ_m from these tests are given in table 7.2. The mean of these values is 27.44° with a standard deviation of 0.74° . This value is approximately 5° lower than the peak static angle of sliding for Darleydale Sandstone.

The corresponding values for the other three rock types are as follows:

	ϕ_m	St.dev.	Peak sliding angle
Portland Limestone	28.69°	1.96°	38°
Permian Sandstone	23.76°	0.86°	32°
Delabole Slate	27.24°	0.82°	31°

It is suggested that the decrease in frictional resistance observed for a sliding block is due to the momentary contact of points on the surface and hence inability of the surfaces to develop a full frictional resistance by adhesion and interlocking. This effect is related to that noted in chapter 5 where surfaces only developed full strength if the sliding plane was taken from horizontal to the angle of sliding, hence allowing the surfaces to bed-in.

7.8 Conclusions from chapter 7

- 1) In these tests, using four different rock types, it has been found that the displacement of a block due to a given vibration record is greater than would be predicted using friction values obtained from 'static' tests.
- 2) The apparent shear strength of the surfaces at the commencement of each cycle of sliding is higher than the equivalent static strength and is dependant upon the rate of loading.
- 3) The frictional resistance during sliding is less than the static frictional resistance.

These conclusions and their implications for seismic design are considered in more detail in the following chapter.